no.3

LIBRARY
FISH & WILDLIFE SERVICE
PACIFIC OCEANIC FISHERY
INVESTIGATIONS

SEARS FOUNDATION FOR MARINE RESEARCH
BINGHAM OCEANOGRAPHIC LABORATORY, YALE UNIVERSITY

APR 23 1953

# JOURNAL OF MARINE RESEARCH

VOLUME XI, 1952

NUMBER 3

ISSUED DECEMBER 31, 1952, NEW HAVEN, CONN., U. S. A.

# JOURNAL OF MARINE RESEARCH

PUBLISHED BY

SEARS FOUNDATION FOR MARINE RESEARCH

BINGHAM OCEANOGRAPHIC LABORATORY, YALE UNIVERSITY

---

BOARD OF EDITORS

*Chairman:* A. E. PARR
*American Museum of Natural History*
*New York*

C. O'D. ISELIN
*Woods Hole Oceanographic Institution*

H. U. SVERDRUP
*Norsk Polarinstitutt*
*Oslo, Norway*

DANIEL MERRIMAN
*Bingham Oceanographic Laboratory*

C.-G. ROSSBY
*Institut für Meteorologi*
*Stockholm, Sweden*

THOMAS G. THOMPSON
*Oceanographic Laboratories*
*University of Washington*

MANAGING EDITOR

YNGVE H. OLSEN
*Bingham Oceanographic Laboratory*
*Yale University*
*New Haven, Conn.*

---

The Journal is normally issued in three numbers per year constituting one volume, except for volume V, published in 1942–1944, and volume VI, published in 1946 and 1947. All the income derived from subscriptions is used solely to increase the volume and improve the quality of the Journal for the benefit of its subscribers and contributors.

**Subscription price three dollars per volume, or one dollar per number. Sverdrup Anniversary Number (Vol. VII, No. 3) available only by purchase of complete Vol. VII at $3.00. Address all communications to the Managing Editor. See inside rear cover for Note to Authors.**

SEARS FOUNDATION FOR MARINE RESEARCH
BINGHAM OCEANOGRAPHIC LABORATORY, YALE UNIVERSITY

JOURNAL OF
MARINE RESEARCH

VOLUME XI 1952 NUMBER 3

# ON THE STATISTICAL DISTRIBUTION OF THE HEIGHTS OF SEA WAVES

By

M. S. LONGUET-HIGGINS

*Trinity College, Cambridge*[1]

## ABSTRACT

The statistical distribution of wave-heights is derived theoretically on the assumptions (a) that the wave spectrum contains a single narrow band of frequencies, and (b) that the wave energy is being received from a large number of different sources whose phases are random. Theoretical relations are found between the root-mean-square wave-height, the mean height of the highest one-third (or highest one-tenth) waves and the most probable height of the largest wave in a given interval of time. There is close agreement with observation.

## 1. INTRODUCTION

At present several different quantities are in use for describing the state of the sea: for example, the mean height of the waves, the root-mean-square height, the height of the "significant" waves (defined by Sverdrup and Munk [1947] as the mean height of the highest one-third of all the waves), the maximum height over a given interval of time, and so on. The purpose of the following is to investigate the relationship of these quantities to one another in some special cases, and especially in the case when the spectrum of the waves consists of a single narrow frequency-band.

[1] The author is indebted to the Commonwealth Fund, New York, for a Fellowship to enable him to study at the Scripps Institution of Oceanography, where this paper was prepared.

For definiteness let us consider the elevation $\zeta$ of the sea surface at a fixed point, given as a function of the time $t$ only. Much of the following, however, will apply to any oscillatory function of a single variable: for example, to the pressure at a point on the bottom, or to the rolling motion of a ship as measured by its angular deflection from the vertical. In general we shall denote by $a$ the amplitude of $\zeta$, which may be defined as half the distance in level between a wave crest and the preceding trough; thus $2a$ equals the wave-height. The period, or interval between successive crests, will be denoted by $\tau$, or $2\pi/\sigma$, where $\sigma/2\pi$ is the frequency. $I$ denotes any interval of the $t$-axis, of length $T$, in which the variable $\zeta$ is under consideration; it is supposed that $T >> \tau$, i. e., the interval contains a large number of complete periods. The successive values of $a$ in the interval $I$ may

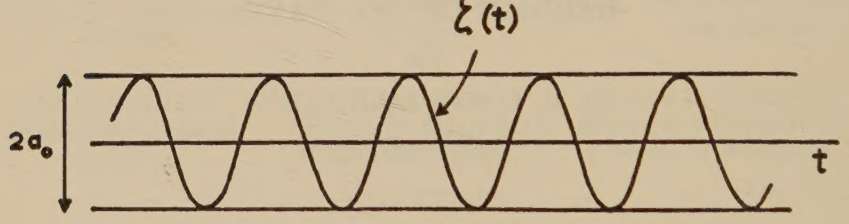


Figure 1. A simple sine-wave: definition of the wave amplitude.

be denoted by $a_1, a_2 \ldots a_N$. If these are arranged in descending order of magnitude, the mean value of the first $pN$ of these, where $p$ is a fraction between 0 and 1, will be denoted by $a^{(p)}$. Thus the amplitude of Sverdrup and Munk's "significant waves" is $a^{(\frac{1}{3})}$. The mean amplitude of all of the waves is $a^{(1)}$. It is clear that $a^{(p)}$ is a decreasing, or at any rate a nonincreasing, function of $p$; and if $a_{max}$ is the maximum value of $a$ in the interval, we have

$$a_{max} \geqslant a^{(p)} \geqslant a^{(1)} . \tag{1}$$

The root-mean-square amplitude $\bar{a}$ is defined by

$$\bar{a}^2 = \frac{1}{N}(a_1^2 + a_2^2 + \ldots + a_N^2) . \tag{2}$$

It may easily be shown that

$$\bar{a} \geqslant a^{(1)} . \tag{3}$$

Since $\bar{a}$ is of physical significance in a wide class of cases, $a^{(p)}$ will normally be expressed in terms of $\bar{a}$. The mode is defined as the most frequently occurring wave amplitude and will be denoted by $\mu(a)$.

*Example 1. Simple sine-wave.* Suppose

$$\zeta = a_0 \cos \sigma t \ ; \tag{4}$$

then we have a simple sine-wave of period $2\pi/\sigma$ and amplitude $a_0$ (see Fig. 1). All the waves are of amplitude $a_0$, and therefore

$$a_{\max} = a^{(p)} = \bar{a} = \mu(a) = a_0 \,. \tag{5}$$

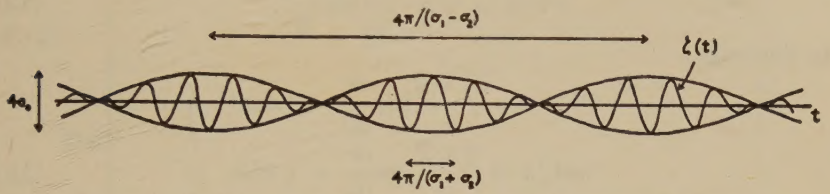


Figure 2. Combination of two sine-waves of slightly different frequency.

*Example 2. Two sine-waves.* Consider the sum of two sine-waves of equal amplitude but of very slightly differing period:

$$\zeta = a_0 \cos \sigma_1 t + a_0 \cos \sigma_2 t \,, \tag{6}$$

say, where $|\sigma_1 - \sigma_2| << |\sigma_1 + \sigma_2|$. We may write

$$\zeta = 2a_0 \cos \frac{\sigma_1 + \sigma_2}{2} t \cos \frac{\sigma_1 - \sigma_2}{2} t \,, \tag{7}$$

showing that the resultant consists of a carrier wave $\cos \frac{\sigma_1 + \sigma_2}{2} t$, whose period is nearly the same as that of the two component waves, modulated by an envelope function $2a_0 \cos \frac{\sigma_1 - \sigma_2}{2} t$, whose period, by hypothesis, is comparatively long (see Fig. 2). The maxima and minima of $\zeta$ occur nearly on the envelope and so are nearly equal in magnitude to the magnitude of the envelope function. In the limit they are distributed at even intervals along the $t$-axis. Taking the interval $0 < t < \pi/(\sigma_1 - \sigma_2)$ as typical, and supposing it contains $N$ waves, we see that the highest $pN$ waves will be contained in the interval $0 < t < p\pi/(\sigma_1 - \sigma_2)$. The mean amplitude $a^{(p)}$ of these is given by

$$\frac{p\pi}{\sigma_1 - \sigma_2} a^{(p)} = \int_0^{p\pi/(\sigma_1 - \sigma_2)} 2a_0 \cos \frac{\sigma_1 - \sigma_2}{2} t \, dt \,, \tag{8}$$

and hence

$$a^{(p)} = 2a_0 \cdot \frac{2}{p\pi} \sin \frac{p\pi}{2} \,. \tag{9}$$

The root-mean-square wave-height is given by

$$\frac{\pi}{\sigma_1 - \sigma_2}\bar{a}^2 = \int_0^{\pi/(\sigma_1-\sigma_2)} 4a_0^2 \cos^2 \frac{\sigma_1 - \sigma_2}{2} t \, dt , \tag{10}$$

and hence

$$\bar{a}^2 = 2a_0 , \qquad \bar{a} = \sqrt{2}\, a_0 . \tag{11}$$

Thus

$$a^{(p)}/\bar{a} = \sqrt{2} \cdot \frac{2}{p\pi} \sin \frac{p\pi}{2} . \tag{12}$$

In particular

$$\left.\begin{aligned} a^{(1/10)}/\bar{a} &= \frac{20\sqrt{2}}{\pi} \sin \frac{\pi}{20} = 1.408 \\ a^{(\frac{1}{6})}/\bar{a} &= \frac{6\sqrt{2}}{\pi} \sin \frac{\pi}{6} = 1.350 \\ a^{(1)}/\bar{a} &= \frac{2\sqrt{2}}{\pi} \sin \frac{\pi}{2} = 0.901 \end{aligned}\right\} \tag{13}$$

$a^{(p)}/\bar{a}$ is plotted against $p$ in Fig. 3. We have also

$$a_{\max} = 2a_0 ; \qquad a_{\max}/\bar{a} = \sqrt{2} . \tag{14}$$

The statistical distribution of the wave amplitudes is evidently the same as that of the envelope function, which is that of the simple cosine curve

$$r = 2a_0 \cos\theta . \tag{15}$$

See Fig. 4. The probability that a point in the interval $0 < \theta < \pi/2$ lies in any given region of width $d\theta$ is $2|d\theta|/\pi$. Hence the probability $P(r)|dr|$ that the function (15) lies between $r$ and $r + dr$ is given by

$$P(r)\,|\,dr\,| = \frac{2}{\pi}\,|\,d\theta\,| . \tag{16}$$

Thus, when $0 < r < 2a$,

$$P(r) = \frac{2}{\pi}\left|\frac{d\theta}{dr}\right| = \frac{2}{\pi}\frac{1}{2a_0 \sin\theta} = \frac{2}{\pi}\frac{1}{(4a_0^2 - r^2)^{\frac{1}{2}}} . \tag{17}$$

Clearly $a$ can never exceed $2a_0$ or $\sqrt{2}\bar{a}$. Hence the probability-distribution $P(r)$ of the wave-height $a$ is given by

$$P(r) = \left\{\begin{aligned} &\frac{2}{\pi}\frac{1}{(2\bar{a}^2 - r^2)^{\frac{1}{2}}}, && (r < \sqrt{2}\bar{a}) \\ &0, && (r > \sqrt{2}\bar{a}) \end{aligned}\right\} \tag{18}$$

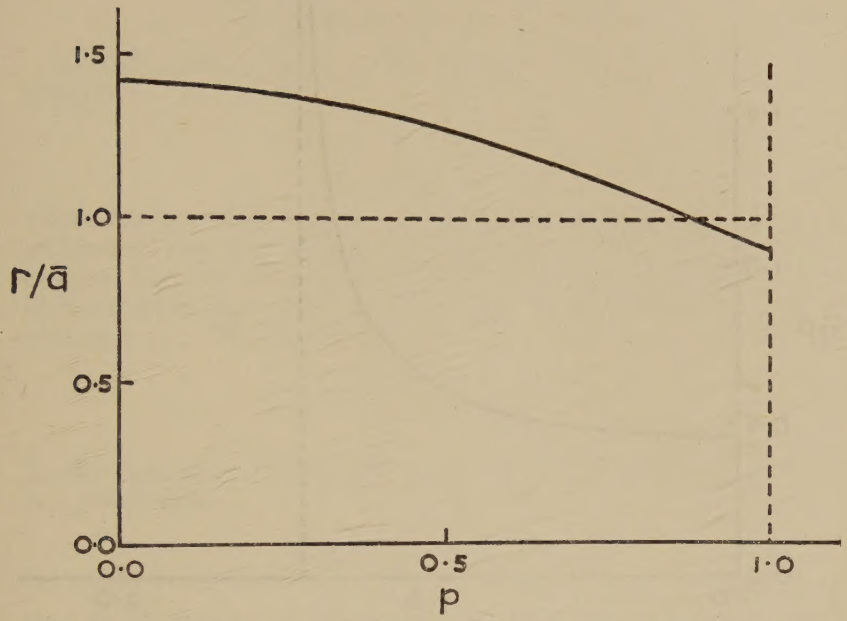


Figure 3. Graph of $a^{(p)}/\bar{a}$ as a function of $p$, for two sine-waves of slightly different frequency.

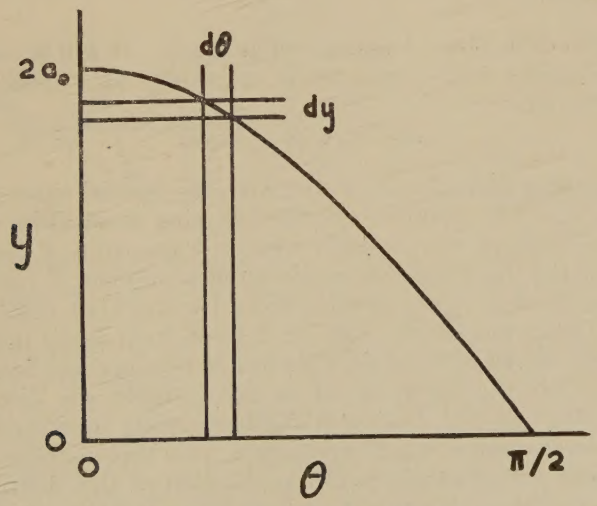


Figure 4. The curve $y = 2a_0 \cos\theta$.

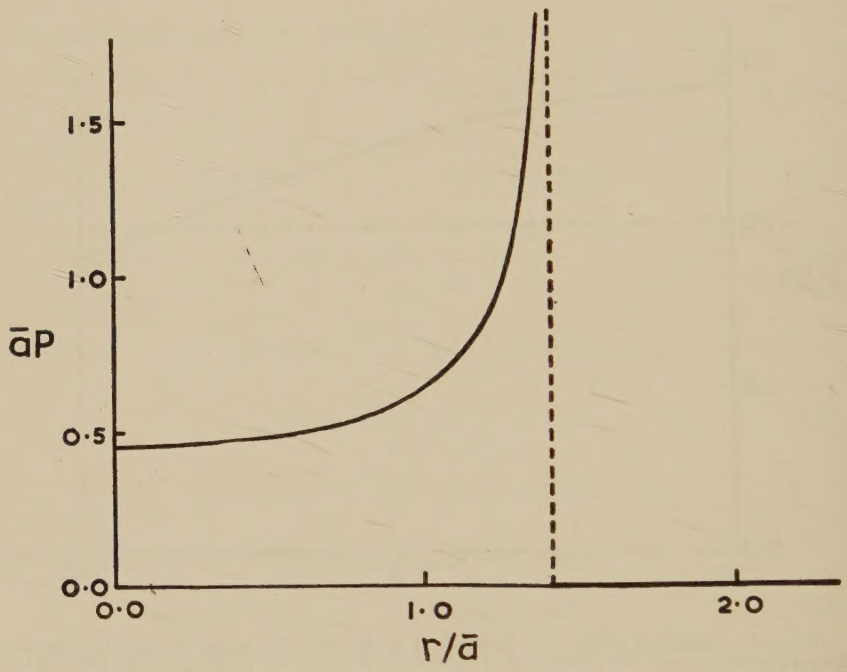


Figure 5. Frequency distribution of the wave amplitude for two sine-waves of slightly different frequency.

The function $\bar{a}P$ is plotted against $r/\bar{a}$ in Fig. 5. It will be seen that $P$ increases steadily with $r$ and tends to infinity as $r$ tends to $\sqrt{2}\bar{a}$. We have therefore

$$\mu(a) = \sqrt{2}\bar{a} = a_{\max} . \tag{19}$$

The foregoing examples, however, are very special cases which are unlikely to occur in practice. In the following we shall be concerned with a more realistic case, namely when the spectrum of the waves is narrow and the disturbance is made up of a number of random contributions. Such a case was considered by Rayleigh (1880) in connection with the amplitude of sound derived from many independent sources, and the theoretical distribution of maxima has been used in acoustics and in the theory of filters (for example, see Rice, 1944–5; Eckart, 1950). Indeed, Barber (1950) has already presented evidence that for waves there is rough agreement with this distribution. We shall consider rather carefully the application of this distribution to sea waves, find the theoretical values of $a^{(p)}/\bar{a}$ and the distribution of $a_{\max}/\bar{a}$, and compare the results with observation.

## 2. A NARROW WAVE-BAND

Let the wave elevation $\zeta$ in any interval $I$ be expressed as a Fourier integral:

$$\zeta = \int_{-\infty}^{\infty} A(\sigma)\, e^{i\sigma t}\, d\sigma\,, \tag{20}$$

where the spectrum function $A(\sigma)$ may be complex and where it is understood that only the real part of the right-hand side is to be taken. Suppose that the spectrum consists of a single narrow frequency-band of wavelength $2\pi/\sigma_0$, say, so that $A(\sigma)$ is appreciable only for values of $\sigma$ near $\sigma_0$. We may write

$$\zeta = e^{i\sigma_0 t} \int_{-\infty}^{\infty} A(\sigma)\, e^{i(\sigma-\sigma_0)t}\, d\sigma\,. \tag{21}$$

In this expression $e^{i\sigma_0 t}$ represents a carrier wave of wavelength $2\pi/\sigma_0$, and the integral

$$B(t) = \int_{-\infty}^{\infty} A(\sigma)\, e^{i(\sigma-\sigma_0)t}\, d\sigma \tag{22}$$

is a slowly varying function which represents the envelope of the waves (see Fig. 6). As in Example 2 above, the maxima and minima

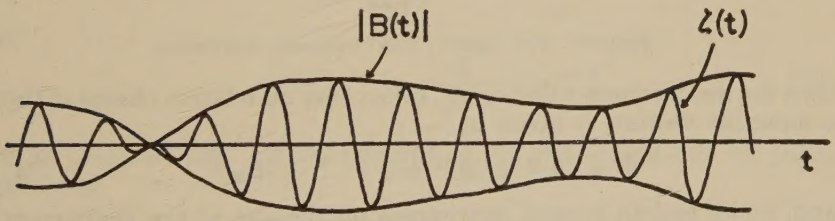


Figure 6. A disturbance $\zeta(t)$ having a narrow frequency band, and its envelope $|B(t)|$.

of $\zeta$ are spaced nearly evenly along the $t$-axis and are approximately equal to the value of $|B|$ at these points. It follows that the probability-distribution of the wave amplitudes is the same as the probability-distribution of $|B|$, which we shall therefore consider.

Now the wave-energy received at any point on the coast will have originated in many different places over a wide area. We may imagine that the generating area of the waves is divided into a large number of different regions, each of which will contribute to the wave-height $\zeta$ and to the envelope function $B$. If each region of the generating area is sufficiently large compared with a wavelength, it may be assumed that the phases of the contributions from different regions are inde-

pendent of one another. Then it is reasonable to assume that $B$ is the sum of a very large number of small components of random phase. The probability-distribution of such a sum, which is known as the "random walk," was found by Rayleigh (1880) and has since been studied by many workers (for references, see Bartels, 1935). If the component vectors are $\boldsymbol{b}_1, \boldsymbol{b}_2, \ldots \boldsymbol{b}_M$, i. e., if

$$B = \boldsymbol{b}_1 + \boldsymbol{b}_2 + \ldots + \boldsymbol{b}_M , \tag{23}$$

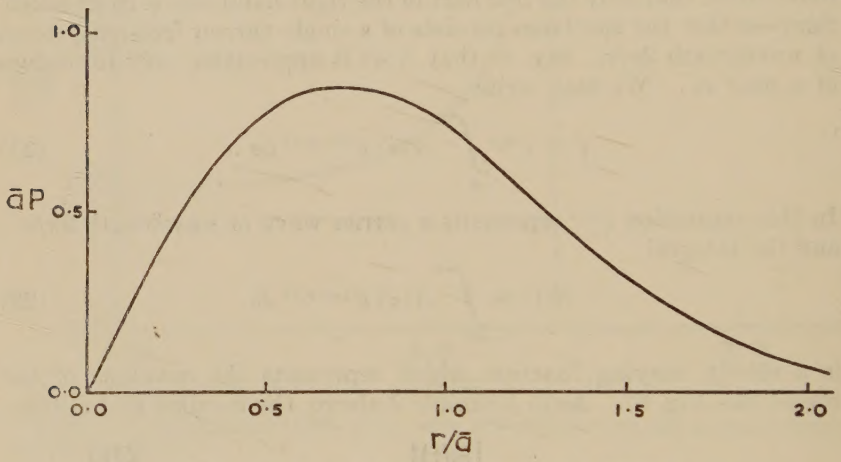


Figure 7. The "random walk" frequency distribution.

then the mean square value of $|B|$, taken over all relative phases of the component vectors, is given by

$$\bar{B}^2 = |\boldsymbol{b}_1|^2 + |\boldsymbol{b}_2|^2 + \ldots + |\boldsymbol{b}_M|^2 , \tag{24}$$

and, under certain general restrictions on the size of the component vectors (see Khintchine, 1933) the probability that $|B|$ lie between $r$ and $r + dr$ is given by

$$P(r)dr = e^{-r^2/\bar{B}^2} \cdot \; 2r/\bar{B}^2 \, dr . \tag{25}$$

Since the probability-distribution of $|B|$ equals that of the $a$'s, we have

$$\bar{B} = \bar{a} , \tag{26}$$

a quantity that can be estimated from observation; no detailed knowledge of the component vectors is required. Thus the probability-distribution of the $a$'s is given by

$$P(r)\, dr = e^{-r^2/\bar{a}^2} \cdot \; 2r/\bar{a}^2 \, dr = - \, de^{-r^2/\bar{a}^2} . \tag{27}$$

The function

$$\bar{a}P(r) = e^{-r^2/\bar{a}^2} \cdot \; 2r/\bar{a} \tag{28}$$

is shown in Fig. 7 (cf. Fig. 5). It will be seen that $P(r)$ is zero when $r = 0$, that it increases to a maximum, and then falls away rapidly for large values of $r/\bar{a}$. The total area under the curve is, of course, unity. The maximum value occurs when $r/\bar{a} = 1/\sqrt{2}$, so that the mode $\mu(a)$ is given by

$$\mu(a)/\bar{a} = \frac{1}{\sqrt{2}} = 0.717 \, . \tag{29}$$

The chance $\varphi(r)$ that $a$ should exceed a certain value $r$ is given by

$$\varphi(r) = \int_r^\infty P(r)dr = e^{-r^2/\bar{a}^2} \, . \tag{30}$$

To find $a^{(p)}$, we note, first, that the proportion $p$ of $a$'s which exceed a certain value $r$ is equal to $\varphi(r)$, so that from (30)

$$p = e^{-r^2/\bar{a}^2} \, ; \qquad r = \left( \log \frac{1}{p} \right)^{\frac{1}{2}} . \tag{31}$$

The mean value $a^{(p)}$ of those $a$'s that are greater than $r$ is given by

$$\varphi(r) \; a^{(p)} = \int_r^\infty r \, P(r) \, dr \tag{32}$$

or

$$e^{-r^2/\bar{a}^2} \, a^{(p)} = - \int_r^\infty r \, d \, e^{-r^2/\bar{a}^2} \tag{33}$$

from (27) and (30). After integrating the right-hand side by parts, we have

$$e^{-r^2/\bar{a}^2} \, a^{(p)} = r \, e^{-r^2/\bar{a}^2} + \int_r^\infty e^{-r^2/\bar{a}^2} \, dr \, , \tag{34}$$

and hence

$$a^{(p)}/\bar{a} = r/\bar{a} + e^{r^2/\bar{a}^2} \int_r^\infty e^{-r^2/\bar{a}^2} \, dr/\bar{a}$$

$$= \left( \log \frac{1}{p} \right)^{\frac{1}{2}} + \frac{1}{p} \int_{\left( \log \frac{1}{p} \right)^{\frac{1}{2}}}^\infty e^{-\theta^2} \, d\theta \tag{35}$$

$$= \left( \log \frac{1}{p} \right)^{\frac{1}{2}} + \frac{1}{p} \frac{\sqrt{\pi}}{2} \left[ 1 - H\left\{ \left( \log \frac{1}{p} \right)^{\frac{1}{2}} \right\} \right] , \tag{36}$$

where $H(\theta)$ is the probability function:

$$H(\theta) = \frac{2}{\sqrt{\pi}} \int_0^{\theta} e^{-\theta^2} d\theta \,. \tag{37}$$

Numerical values of $a^{(p)}/\bar{a}$ are given in Table I for some representative values of $p$. In particular, the mean $a^{(1)}$ is given by

$$a^{(1)}/\bar{a} = \frac{\sqrt{\pi}}{2} = 0.886 \,. \tag{38}$$

TABLE I. Representative Values of $a^{(p)}/\bar{a}$ in the Case of a Narrow Wave Spectrum

| $p$ | $a^{(p)}/\bar{a}$ | $p$ | $a^{(p)}/\bar{a}$ |
|---|---|---|---|
| 0.01 | 2.359 | 0.4 | 1.347 |
| 0.05 | 1.986 | 0.5 | 1.256 |
| 0.1 | 1.800 | 0.6 | 1.176 |
| 0.2 | 1.591 | 0.7 | 1.102 |
| 0.25 | 1.517 | 0.8 | 1.031 |
| 0.3 | 1.454 | 0.9 | 0.961 |
| 0.3333 | 1.416 | 1.0 | 0.886 |

The second moment of the distribution about the origin being $\bar{a}^2$, by definition, we have for the second moment about the mean:

$$[\delta(a)]^2 = \bar{a}^2 - a^{(1)2} = \bar{a}^2 \left(1 - \frac{\pi}{4}\right). \tag{39}$$

Thus the standard deviation $\delta(a)$ is given by

$$\delta(a)/\bar{a} = \left(1 - \frac{\pi}{4}\right)^{\frac{1}{2}} = 0.453 \,. \tag{40}$$

$a^{(p)}/\bar{a}$ is shown as a function of $p$ in Fig. 8, which may be compared with Fig. 3. An asymptotic formula for $a^{(p)}/\bar{a}$ when $p$ approaches zero is found by further integration by parts in equation (35):

$$a^{(p)}/\bar{a} = \left(\log \frac{1}{p}\right)^{\frac{1}{2}} + \frac{1}{2}\left(\log \frac{1}{p}\right)^{-\frac{1}{2}} - \frac{1}{2} \cdot \frac{3}{2}\left(\log \frac{1}{p}\right)^{-\frac{3}{2}} + \frac{1}{2} \cdot \frac{3}{2} \cdot \frac{5}{2}\left(\log \frac{1}{p}\right)^{-\frac{5}{2}} \cdots\cdots \tag{41}$$

Thus, in Fig. 8, as $p$ tends to 0, $a^{(p)}/\bar{a}$ tends to infinity logarithmically. However, for the validity of this result it is essential that the fraction of the sample containing the highest $pN$ wave amplitudes $a$ shall not be too small; otherwise the present approximation will not hold.

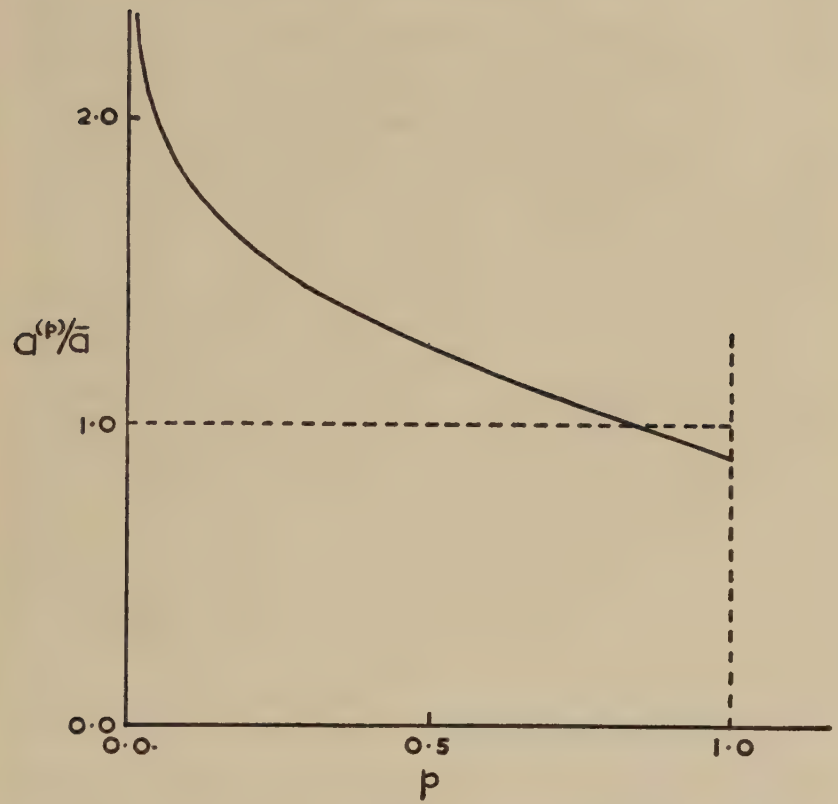


Figure 8. Graph of $a^{(p)}/\bar{a}$ as a function of $p$, for the narrow frequency band.

Suppose, for example, that we wish to find the expectancy $E(a_{\max})$ of the highest wave in an interval containing $N$ waves. An approximate answer might be obtained by setting $p = 1/N$ and finding $a^{(1/N)}$. But this answer will not be exactly correct; for $a^{(1/N)}$ in fact represents the mean height of the $1/N$th highest waves in a large sample, say a sample of size $mN$ obtained by collecting together $m$ samples, each containing $N$ wave amplitudes. The $m$ highest waves may not be distributed evenly, one in each of the samples; and if not, the mean of the highest waves, one from each group, will clearly be less than the mean of the $m$ highest from all $mN$ wave amplitudes together. Hence we see that the expected value of $a_{\max}$ must be somewhat less than $a^{(1/N)}$.

Of course the ratios $a^{(p)}/\bar{a}$ found above refer to the total statistical "population" of wave amplitudes, or at least to a sample of theoreti-

cally infinite size selected at random from this population. In practice we have to consider samples of finite size $N$. For each ratio such as $a^{(p)}/\bar{a}$, theoretically there will be a corresponding probability-distribution depending on $N$. The expectancy value and the most probable value of $a^{(p)}/\bar{a}$ and of $a^{(p_1)}/a^{(p_2)}$ (where $p_1$ and $p_2$ are two different values of $p$) will differ slightly from the corresponding (exactly defined) values for the whole population. But when $N$ and $pN$ are large, these differences can be expected to be very small, and in the present discussion they will be neglected.

On the other hand, the expectancy of $a_{\max}$, the maximum wave amplitude in a sample, depends fundamentally on the size of the sample.

One further point may be mentioned here. Strictly the analysis is valid only if the sampling of the wave amplitudes is random. In fact the sample consists of $N$ consecutive wave amplitudes; since the envelope function varies slowly, there must be some correlation between members of the sample, especially when the spectrum is narrow. This may affect slightly the probability-distribution of, say, $a^{(p)}/\bar{a}$; but provided the record contains more than one or two wave groups, the effect of the "grouping" can be expected to be very small. Fluctuation of the envelope function may even act as a "randomising" process and may lead to observed ratios in closer agreement with the theoretical ratios than expected. At all events, the effect of "grouping" will be ignored in the present paper.

## 3. THE MAXIMUM WAVE AMPLITUDE

The probability-distribution of $a_{\max}$ may be derived as follows: The chance that any particular one of the $a$'s in the sample should be less than $r$, say, is

$$\int_0^r P(r)\,dr = 1 - \varphi(r)\,, \tag{42}$$

where $\varphi$ is given by equation (30). The chance that every $a$ in the sample shall be less than $r$ is therefore $(1 - \varphi)^N$; and the chance that at least one $a$ shall exceed $r$ is $1 - (1 - \varphi)^N$. The chance that the maximum $a$ shall lie in the interval $(r, r + dr)$ is the chance that at least one $a$ shall exceed $r$, minus the chance that at least one $a$ shall exceed $r + dr$, that is,

$$-\,d\,[1 - (1 - \varphi)^N]\,, = d\,(1 - \varphi)^N\,, \tag{43}$$

or

$$N(1 - \varphi)^{N-1} P\,dr\,, \tag{44}$$

since

$$\frac{d\varphi}{dr} = -\,P\,. \tag{45}$$

Thus the probability-distribution of $a_{\max}$ is

$$N(1-\varphi)^{N-1}P\,. \tag{46}$$

The expectation $E(a_{\max})$ of the maximum is given by

$$E(a_{\max}) = -\int_0^\infty r\,d\,[1-(1-\varphi)^N]\,. \tag{47}$$

On integrating by parts and assuming

$$r\,[1-(1-\varphi)^N] \to 0 \tag{48}$$

when $r \to \infty$ , we have

$$E(a_{\max}) = \int_0^\infty [1-(1-\varphi)^N]\,dr\,. \tag{49}$$

On substitution from (30) we have

$$E(a_{\max})/\bar{a} = \int_0^\infty [1-(1-e^{-r^2/\bar{a}^2})^N]\,dr/\bar{a} \tag{50}$$

$$= \frac{1}{2}\int_0^\infty [1-(1-e^{-\theta})^N]\,\theta^{-\frac{1}{2}}d\theta\,. \tag{50a}$$

For small or moderately large values of $N$, the above integral can be evaluated by a direct expansion, using the binomial theorem; thus

$$E(a_{\max})/\bar{a} =$$

$$\frac{1}{2}\int_0^\infty \left[Ne^{-\theta} - \frac{N(N-1)}{1.2}e^{-2\theta} + \ldots (-)^{NH}e^{-N\theta}\right]\theta^{-\frac{1}{2}}d\theta\,, \tag{51}$$

and since

$$\int_0^\infty e^{-n\theta}\,\theta^{-\frac{1}{2}}d\theta = n^{-\frac{1}{2}}\left(-\frac{1}{2}\right)! = \left(\frac{\pi}{n}\right)^{\frac{1}{2}}, \tag{52}$$

we have

$$E(a_{\max})/\bar{a} = \frac{\sqrt{\pi}}{2}\left[\frac{N}{\sqrt{1}} - \frac{N(N-1)}{1.2}\frac{1}{\sqrt{2}} + \ldots (-)^{N+1}\frac{1}{\sqrt{N}}\right]. \tag{53}$$

Table II gives the exact values of the integral for $N = 1, 2, 5, 10$ and 20. However, we are chiefly interested in values of $N$ of the order of 50 or more, for which the binomial coefficients in (53) become so large that computation by means of that expression becomes impracticable.

An asymptotic expression for large values of $N$ may be found as follows: write

$$\theta_0 = \log N\,; \qquad e^{-\theta_0} = \frac{1}{N}\,; \qquad \theta = \theta_0 + \theta'\,, \tag{54}$$

say, then

$$(1 - e^{-\theta})^N = \left(1 - \frac{e^{-\theta'}}{N}\right)^N \doteq e^{-e^{-\theta'}}\,, \tag{55}$$

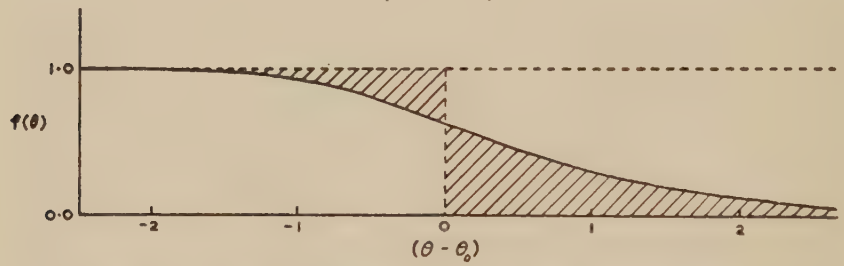


Figure 9. Graph of the function $f(\theta) = (1 - e^{-\theta})^N$ when $N$ is large.

with errors of order $1/N$. Thus we see that the first function in the integrand of (43), i. e.,

$$f(\theta) = 1 - (1 - e^{-\theta})^N, \tag{56}$$

has a rather sudden drop from 1 to 0 in the neighborhood of $\theta_0$ (see Fig. 9). We have, therefore,

$$I = \frac{1}{2}\int_0^{\theta_0} \theta^{-\frac{1}{2}}\, d\theta + R \tag{57}$$

$$= \theta_0^{\frac{1}{2}} + R\,,$$

where $R$ is a remainder of order $\theta_0^{-\frac{1}{2}}$ at most; in fact

$$R = \frac{1}{2}\,\theta_0^{-\frac{1}{2}}\left[-\int_{-\infty}^{0} e^{-e^{-\theta'}} d\theta' + \int_0^{\infty} (1 - e^{-e^{-\theta'}}) d\theta'\right] + R'$$

$$= \frac{1}{2}\,\theta_0^{-\frac{1}{2}}\left[-\int_1^{\infty} e^{-\alpha}\frac{d\alpha}{\alpha} + \int_0^{1} (1 - e^{-\alpha})\,\frac{d\alpha}{\alpha}\right] + R'$$

$$= \tfrac{1}{2}\gamma\,\theta_0^{-\frac{1}{2}} + R', \tag{58}$$

where $R'$ is of order $\theta_0^{-\frac{1}{2}}$ at most and $\gamma$ is Euler's constant ($= 0.5772{,}2$; see Whittaker and Watson, 1950: 236). Thus

$$E(a_{\max}) \,/\, \bar{a} = (\log N)^{\frac{1}{2}} + \frac{1}{2}\,\gamma\,(\log N)^{-\frac{1}{2}} + 0\,(\log N)^{-\frac{1}{2}}\,. \tag{59}$$

TABLE II. VALUES OF $E(a_{max})/\bar{a}$ AND $\mu(a_{max})/\bar{a}$ FOR DIFFERENT VALUES OF $N$, FOR A NARROW SPECTRUM

| $N$ | $(\log N)^{\frac{1}{2}}$ | $E(a_{max})/\bar{a}$ exact expression | $E(a_{max})/\bar{a}$ asymptotic expression | $\mu(a_{max})/\bar{a}$ |
|---|---|---|---|---|
| 1 | 0.000 | 0.886 | —— | 0.707 |
| 2 | 0.833 | 1.146 | —— | 1.030 |
| 5 | 1.269 | 1.462 | —— | 1.366 |
| 10 | 1.517 | 1.676 | 1.708 | 1.583 |
| 20 | 1.731 | 1.870 | 1.898 | 1.778 |
| 50 | 1.978 | —— | 2.124 | 2.010 |
| 100 | 2.146 | —— | 2.280 | 2.172 |
| 200 | 2.302 | —— | 2.426 | 2.323 |
| 500 | 2.493 | —— | 2.609 | 2.509 |
| 1,000 | 2.628 | —— | 2.738 | 2.642 |
| 2,000 | 2.757 | —— | 2.862 | 2.769 |
| 5,000 | 2.918 | —— | 3.017 | 2.929 |
| 10,000 | 3.035 | —— | 3.130 | 3.044 |
| 20,000 | 3.147 | —— | 3.239 | 3.155 |
| 50,000 | 3.289 | —— | 3.377 | 3.296 |
| 100,000 | 3.393 | —— | 3.478 | 3.400 |

The above equation may be compared with equation (41) for $a^{(p)}/\bar{a}$ when $p = 1/N$. We see that $E(a_{\max})$ differs from $a^{(1/N)}$ in the second term of the asymptotic expansion. Since $\frac{1}{2}\gamma = 0.28861$, we have $E(a_{\max}) < a^{(1/N)}$ as expected. For large $N$, however, $E(a_{\max})$ still increases like $(\log N)^{\frac{1}{2}}$ and therefore tends to infinity with the length of the interval, though very slowly. Values of the asymptotic expression for $E(a_{\max})/\bar{a}$ are given in Table II for values of $N$ ranging from 10 to 100,000. It will be seen that in this range $E(a_{\max})/\bar{a}$ increases only from about 1.7 to about 3.5. The asymptotic expression may be compared with the exact expression for $N = 10$ and 20. The differences in the two cases are 0.032 and 0.028 respectively, or about 2%. For $N \geqslant 50$ the error in the asymptotic expression is almost certainly less than 0.03; for large values of $N$ the error may be expected to diminish proportionally to $(\log N)^{-\frac{1}{2}}$.

The "most probable" value of $a_{\max}$, which we shall denote by $\mu(a_{\max})$, is given simply by the maximum value of the probability-distribution (46), i. e., the maximum of

$$N(1 - e^{-r^2/\bar{a}^2})^{N-1} e^{-r^2/\bar{a}^2} \cdot 2r/\bar{a}\,. \tag{60}$$

Writing

$$\theta = r^2/\bar{a}^2\,, \tag{61}$$

we see that we must have

$$\frac{d}{d\theta}\left[\theta^{\frac{1}{2}} e^{-\theta}(1 - e^{-\theta})^{N-1}\right] = 0\,, \tag{62}$$

and hence

$$\frac{1}{2\theta} - 1 + \frac{(N-1)e^{-\theta}}{1-e^{-\theta}} = 0 \tag{63}$$

or

$$Ne^{-\theta} = 1 - \frac{1}{2\theta}\left(1 - e^{-\theta}\right) \tag{64}$$

or

$$\theta = \log N - \log\left[1 - \frac{1}{2\theta}(1 - e^{-\theta})\right] \tag{65}$$

$$= \log N + 0\left(\frac{1}{\theta}\right) \tag{66}$$

when $N$ is large. Thus

$$\theta = \log N + 0\,(\log N)^{-1}, \tag{67}$$

and the most probable value of $a_{\max}$ is given by

$$\mu(a_{\max})/\bar{a} = \theta^{\frac{1}{2}} = (\log N)^{\frac{1}{2}} + 0(\log N)^{-\frac{1}{2}}. \tag{68}$$

Thus there is no term in $(\log N)^{-\frac{1}{2}}$. Starting with the approximate value $(\log N)^{\frac{1}{2}}$, one may find closer approximations to $\mu(a_{\max})/\bar{a}$ by applying Newton's method of successive approximation (see, for example, Whittaker and Robinson, 1932: 84) in equation (65). Values of $\mu(a_{\max})/\bar{a}$ so found are given in the last column of Table II.

The chance that $a_{\max}$ shall not exceed $(\log N)^{\frac{1}{2}}$ by more than a given amount may be found similarly. We have seen that the probability-distribution of $a_{\max}$ is given by

$$\frac{d}{dr}(1-\theta)^N = \frac{d}{dr}(1 - e^{-r^2/\bar{a}^2})^N. \tag{69}$$

If we define $r_0$ by the equations

$$r_0^2/\bar{a}^2 = \theta_0 = \log N\,;\; e^{-r_0^2/\bar{a}^2} = \frac{1}{N}\,, \tag{70}$$

we have

$$\frac{d}{dr}\left(1 - \frac{e^{-(r^2-r_0^2)/\bar{a}^2}}{N}\right)^N = \frac{d}{dr}\,e^{-e^{-(r^2-r_0^2)/\bar{a}^2}} \tag{71}$$

approximately. The probability that $a$ will be less than $r$ is therefore

$$e^{-e^{-(r^2-r_0^2)/\bar{a}^2}}, \tag{72}$$

and the probability that $a$ will be greater than $r$ is

$$1 - e^{-e^{-(r^2-r_0^2)/\bar{a}^2}}. \tag{73}$$

## 4. DISCUSSION

The chief assumptions used in the derivation of the theoretical distribution $P(r)$ in sections 2 and 3 are: (a) that the frequency spectrum consist of a single narrow frequency band; and (b) that the waves be considered as the sum of a large number of contributions, all of about the same frequency, and of random phase. Let us consider under what conditions these assumptions should be satisfied.

In the first place, the analysis will not apply to regular trains of waves produced by a simple organized mechanism: for example, the waves generated by a paddle in a model wave tank, or the transverse waves produced by a ship; or the wave-height distribution resulting from the interference of two wave trains of the same amplitude but of slightly differing wavelength, as in Example 2 (p. 247). In the open sea such examples constitute very special and most unlikely cases.

The present analysis is meant to apply to wind-generated waves. Since the dimensions of a storm area are large compared with the wavelengths we are considering, it is fairly safe to suppose that the phases of contributions from different parts of the storm area are random. However, the range of frequencies may not be narrow; if there are two distinct sources of wave-energy, for example a distant storm and local winds, there may well be two distinct frequency-bands in the spectrum. The most satisfactory conditions would be represented by a single storm at a great distance (compared with the dimensions of the storm); for, in the course of propagation, different frequencies in the spectrum, being propagated with different velocities, will become spread out in space, and over a short interval of time only a narrow range will be present. It must be assumed that the time of recording is not too long, so that in this time the frequency and amplitude of the waves do not change significantly. On the other hand the time must be long enough to ensure that the sample of wave-heights is sufficiently representative; this requires that at least several "groups" of waves be included in the record.

The method of recording may affect the apparent frequency spectrum of the waves. For example, if the waves are recorded by measurement of pressure on the bottom, as is now usual, the high frequencies, which are attenuated rapidly with depth, will be damped out relative to the lower frequencies, and the corresponding frequency spectrum will therefore be narrower. Hence the present analysis may apply more closely to a record of pressure on the bottom than to the actual surface elevation. In fact, the free surface, if viewed very closely, will usually show a large number of short steep waves, which may constitute maxima and minima of the wave elevation but which

are not normally of interest to us; for example, they would not affect the rolling or heaving motion of a ship. Strictly speaking, we should consider only that modification of the spectrum which is relevant to the purpose in hand. A ship itself acts as a resonant filter, which will amplify those components in the spectrum which are close to its natural period. The present analysis, therefore, might very well be applied to the angular deflection of a ship's mast from the vertical; from an analysis of the rolling motion over a few minutes, one could easily compute the maximum roll that is likely to be encountered during, say, the next hour, assuming that the sea conditions remained constant; for, in the notation in Sections 2 and 3, one could estimate $\bar{a}$ with fair accuracy from observation over the shorter interval and hence find $E(a_{\max})$ or $\mu(a_{\max})$ over the proposed longer interval.

However, an important restriction should be mentioned here. One of the conditions implied in assumption (b) above is that the contributions from different parts of the generating area should be superposable; that is, the mechanical system we are dealing with should be linear. This assumption can be shown to be valid for low waves in deep water; but clearly it will not hold for waves approaching the maximum height. For this reason the analysis could not be applied to surf or to waves in the open sea which are nearly at their maximum height. Nor could it be applied to the rolling motion of a ship when this is large enough for nonlinear terms to become important or when the rolling is so great that the ship may capsize.

With these restrictions in mind let us compare some previous observations with the theoretical results of Sections 2 and 3.

## 5. COMPARISON WITH OBSERVATION

Munk (1944),[2] in an analysis of wave records taken at the Scripps Institution, California, compared the mean height $H^{(3/10)}$ of the highest 30% of the waves with the mean height $H^{(1)}$ of all of the waves. He found

$$\frac{H^{(3/10)}}{H^{(1)}} = \frac{0.49}{0.32} = 1.53 .$$

The theoretical value from Table I is given by

$$\frac{a^{(3/10)}}{a^{(1)}} = \frac{a^{(3/10)}/\bar{a}}{a^{(1)}/\bar{a}} = \frac{1.454}{0.886} = 1.64 .$$

Seiwell (1948) found that in two different localities in the Atlantic (off Cuttyhunk Island and off Bermuda) the ratio of $a^{(\frac{1}{3})}$ to $a^{(1)}$ was

[2] See also Snodgrass (1951) where these and other unpublished observations are summarized.

1.57. Putz (1950) studied 25 wave records from five different localities; the mean values of the ratios $a^{(\frac{1}{3})}/a^{(1)}$ can be found from table 1 of his paper. They are respectively 1.59 (Oceanside, 4 records); 1.66 (Point Sur, 15 records); 1.66 (Hecata Head, 2 records); 1.55 (Guam, 3 records) and 1.54 (Point Arguello, 1 record). The mean of Putz's observations, weighted according to the number of records considered, is 1.63. The theoretical value, from Table I of this paper, is given by

$$\frac{a^{(\frac{1}{3})}}{a^{(1)}} = \frac{1.416}{0.886} = 1.60\,,$$

which is in fairly close agreement.

Wiegel (1949) has studied wave records from three different localities off the Pacific Coast of the United States. He found, in the three cases, that

$$\frac{a^{(1/10)}}{a^{(1)}} = 1.27,\ 1.30,\ 1.30 \text{ (mean value } 1.29)\,.$$

The individual estimates showed little scatter. Wiegel remarks, "Even more surprising was the fact that almost every point was within plus or minus ten per cent of this value (1.29)." The theoretical value, from Table I, is given by

$$\frac{a^{(\frac{1}{3})}}{a^{(1)}} = \frac{1.800}{1.416} = 1.27\,,$$

which again is in quite close agreement.

Wiegel also compared the maximum wave from three 20–minute records each day with the mean height of the highest one-third waves. His observed values were equivalent to

$$\frac{E(a_{\max})}{a^{(\frac{1}{3})}} = 1.85,\ 1.91,\ 1.85 \text{ (mean value } 1.87)\,.$$

Assuming a mean wave period of 12 seconds, we have

$$N = \frac{60 \text{ minutes}}{12 \text{ seconds}} = 300\,,$$

for which we find from the asymptotic formula (59):

$$\frac{E(a_{\max})}{\bar{a}} = 2.504\,.$$

Thus, theoretically,

$$\frac{E(a_{\max})}{a^{(\frac{1}{3})}} = \frac{2.504}{1.416} = 1.77\,.$$

A possible explanation of the observed value of $E(a_{max})/a^{(\frac{1}{3})}$ being greater than the theoretical value is as follows. Suppose that during the day the state of the sea, as represented by the r. m. s. wave amplitude $\bar{a}$, underwent a change. If, during one of the three 20-minute records, the r. m. s. wave amplitude is much larger than, say twice, that in the other two, then the maximum wave amplitude will almost certainly be found in that record, and the expected value of the maximum will not be much less than twice the expected value if the wave characteristics had not changed; for $E(a_{max})/\bar{a}$ is not much different for a 20-minute interval than for a 60-minute interval. On the other hand, $a^{(\frac{1}{3})}$ will be multiplied by approximately 4/3. Therefore $E(a_{max})/\bar{a}$ will be increased by about $2 \div 4/3$ or by 3/2. The same tendency is true in general.

Darbyshire (1953) has shown that in a 20-minute wave record the maximum wave-height is about twice the "equivalent wave-height," which is defined by him as the height of the uniform train of waves which would have the same total energy as the actual waves. On our present assumption that the spectrum of the waves contains only a single narrow band, the equivalent wave-height equals the root-mean-square wave height $\bar{a}$; for, each wave in the record is approximately a sine-wave of the same length, and the energy per wavelength is proportional to $a_i^2$. It may be more appropriate, in this case, to consider the most probable value $\mu(a_{max})$ of the highest wave rather than the expectancy $E(a_{max})$. For a mean wave period of 12 seconds we should have

$$N = \frac{20 \text{ minutes}}{12 \text{ seconds}} = 100 ,$$

and so from Table II

$$\mu(a_{max})/\bar{a} = 2.17.$$

However, we see from Table II that $E(a_{max})$ is only slightly greater. For longer wave periods, $N$, and therefore $\mu(a_{max})/\bar{a}$, would be slightly less; the rather slow change in $\mu(a_{max})$ with $N$ would account for the success of the empirical rule irrespective of the period of the waves.

In examples quoted above, the discrepancy between theory and observation is in all cases less than 8%, and in some cases it is smaller still. In view of the somewhat strict assumptions made in deriving the theoretical probability-distribution, this agreement is surprisingly close; and it may indicate that the probability-distribution does not depend very critically upon the narrowness of the wave spectrum. For most practical purposes the theoretical values of $a^{(p)}/\bar{a}$ and $E(a_{max})/\bar{a}$ can be used with confidence; thus, if one of the quantities $\bar{a}$, $a^{(1)}$, $a^{(\frac{1}{3})}$, $a^{(1/10)}$ or $E(a_{max})$ is known, the others may be estimated immediately.

The present discussion suggests that waves much higher than the average are likely to be extremely rare, for a given state of the sea. Table II shows that even in a time interval containing 100,000 waves, which for 10-second waves would be about 11½ days, the most probable value of the highest wave is less than 3½ times the root-mean-square value; of course it is unlikely that the waves would remain statistically constant throughout this interval. Equation (73) also shows that there is an extremely small chance that the most probable value of $a_{max}$ will be greatly exceeded. The general conclusion then appears that changes in the strength of the wind or other generating forces are more important in producing variability in the wave amplitude than is the statistical variation of the waves at any one time.

## REFERENCES


Barber, N. F.

1950. Ocean waves and swell. Lecture published by Institution of Electrical Engineers, London. 22 pp.

Bartels, J.

1935. Random fluctuations, persistence and quasi-persistence in geophysical and cosmical periodicities. Terr. Magn. atmos. Elect., *40;* 1–60.

Darbyshire, J.

1953. The generation of waves by wind. Philos. Trans., A. (in press).

Eckart, C. H. (ed.)

1950. Principles of underwater sound. National Defense Research Council, Summary Technical Reports, Division 6, vol. 7.

Khintchine, A.

1933. Asymptotische Gesetze der Wahrscheinlichkeitsrechnung. Ergebn. Math., *2* (4): 1–77; Berlin, Julius Springer.

Munk, W. H.

1944. Proposed uniform procedure for observing waves and interpreting instrument records. Scripps Institution of Oceanography, Wave Report 26 (unpubiished).

Putz, R. R.

1950. Wave height variability; prediction of distribution function. Institute of Engineering Research, Berkeley, Technical Report HE-116-318 (unpublished).

Rayleigh, Lord

1880. On the resultant of a large number of vibrations of the same pitch and of arbitrary phase. Phil. Mag., *10:* 73–78.

Rice, S. O.

1944–45. The mathematical analysis of random noise. Bell Syst. tech. J., *23:* 282–332; *24:* 46–156.

Seiwell, H. R.

1948. Results of research on surface waves of the western North Atlantic. Pap. phys. Oceanogr. Met., *10* (4).

Snodgrass, F. E.
1951. Wave recorders. Proc., 1st Conference on Coastal Engineering, pp. 69–81, published by Council on Wave Research, University of California, 1951 (ed., J. W. Johnson).
Sverdrup, H. U. and W. H. Munk
1947. Wind, sea and swell: theory of relations for forecasting. Report N. 601, U. S. Navy Hydrographic Office.
Whittaker, E. T. and G. Robinson
1932. Calculus of Observations. 2nd ed., Blackie, London. 395 pp.
Whittaker, E. T. and G. N. Watson
1950. Modern Analysis. 4th ed., Cambridge University Press. 608 pp.
Wiegel, R. L.
1949. An analysis of data from wave recorders on the Pacific Coast of the United States. Trans. Amer. geophys. Un., *30:* 700–704.

# THE SURFACE LAYER OF THE GULF STREAM AND ADJACENT WATERS[1]

By

WILLIAM L. FORD and A. R. MILLER

## ABSTRACT

This paper presents a description of the Gulf Stream system between Cape Hatteras and 63° W. Long. and gives a qualitative analysis of the water masses in the surface layer on the basis of observations taken from November 15 to December 6, 1948. The edge of the Stream was explored for 1,050 miles of its length. The meanderings of the Stream and its tendency to develop large eddies are demonstrated. Of special note was the 90° change in direction of the mean axis of a 150-mile segment of the Stream within a period of two weeks. Surface current velocities are given for many points; flows in excess of 5.5 knots were found on several occasions. By means of a T-S analysis applicable during the period of the cruise, the surface layer of the system is described in terms of four water types. The occurrence and interplay of these water types are discussed. Noteworthy features are (a) the presence of Shelf water at certain points along the edge of the Stream and (b) the modification of the surface layer of the Stream by the addition of Sargasso water, with no evidence of the absorption of Slope waters.

## INTRODUCTION

Although there have been many investigations of the Gulf Stream, it is only recently that detailed quasisynoptic surveys have been possible. This new approach is based on rapid measuring devices developed during World War II—the Bathythermograph (BT), the Sea Sampler (Spilhaus and Miller, 1948) and the Salinity-Temperature-Depth Recorder (Jacobsen, 1948; Ford, 1949) together with Loran which provides the necessary accuracy in navigation. The first surveys of the Stream with the BT and Sea Sampler were made by Spilhaus (1940, 1941), though without the benefit of Loran which had not yet been perfected. Following the war, rapid detailed surveys of the Gulf Stream were made using both the BT and Loran (Fuglister and Worthington, 1947; Iselin and Fuglister, 1948). These studies revealed that the highest current velocities tend to be associated with a sharp change in the temperature structure in the upper layers of the Gulf Stream and that the path of the Stream is of a meandering and variable nature.

[1] This paper is a joint contribution from the Naval Research Establishment of the Defence Research Board of Canada, c/o Fleet Mail Office, Halifax, N. S. (Wm. L. Ford) and the Woods Hole Oceanographic Institution, Woods Hole, Mass. (A. R. Miller). Contribution No. 619 from the Woods Hole Oceanographic Institution.

In our studies the above technique was extended to include the use of the Sea Sampler and the Salinity-Temperature-Depth Recorder. The general objective was to enlarge our meagre knowledge of the Stream by examining its meanderings and structure in as much detail and over as great a portion of its length as time would permit.

## DATA

The area covered by the cruise from November 15 to December 6, 1948 is shown in Fig. 1. In all, 1,050 miles of the Stream were traced, 180 miles in the first survey and 870 in the second. Bathythermograms (660) were usually taken at half-hour intervals and to depths of 700–800 feet. Forty-three Sea Sampler lowerings yielded temperature traces to 450 feet together with an average of 10 salinity samples at each lowering to a depth of 320 feet. On the passage from Bermuda to Norfolk, Sea Sampler observations were made every four hours. Along the zig-zag route from Norfolk to Halifax, subsurface sampling was done usually on either side of the left edge of the Gulf Stream. Information on temperature-salinity (T-S) relationships obtained in this manner was supplemented by the continuous record of surface temperature and salinity obtained with a Salinity-Temperature-Depth Recorder (STD). Loran fixes were taken every 15 minutes, thus providing an unusually good body of navigational data.

The "inshore" or left edge of the Gulf Stream, looking in the direction of flow, is usually a sharp and well defined boundary characterized by an abrupt downward slant of the isotherms (see Fig. 4). In this paper the edge of the Stream is defined as the position at which the 65° isotherm reached a depth of 150 feet. The location of the inshore edge, and hence the path of the Stream, as found at various stages of this cruise is shown in Fig. 1 by the heavy line. The Stream itself lies to the right of this edge and flows more or less parallel to it. There is no well defined edge on the right-hand side.

The paths of the Stream shown in Fig. 1 tend to confirm the observations of Iselin and Fuglister (1948) and Church (1937) that the current not only meanders but that the meanderings develop progressively eastward from Cape Hatteras. Fig. 1 also provides some evidence on the rate of change of the Stream's path in that the mean axis of a 150-mile segment of it is shown as having changed direction by 90° within a period of two weeks.

The large swing east of 65° W. Long. is of particular interest. It is unfortunate that bad weather and a dwindling fuel supply made it necessary to terminate the survey without a full investigation of what appeared to be a large anticyclonic eddy centered on 64° W. Long.

and 39° N. Lat. In the centre of this eddy there is a submarine mountain that rises 10,000 feet above the surrounding ocean bed to within 6,000 feet of the surface. It is suggested that this submarine mountain may be a cause of large scale eddies in the Stream. A review of available data suggests that well developed meanders and probably eddies exist more often than not in this area (Iselin, 1936; Fuglister

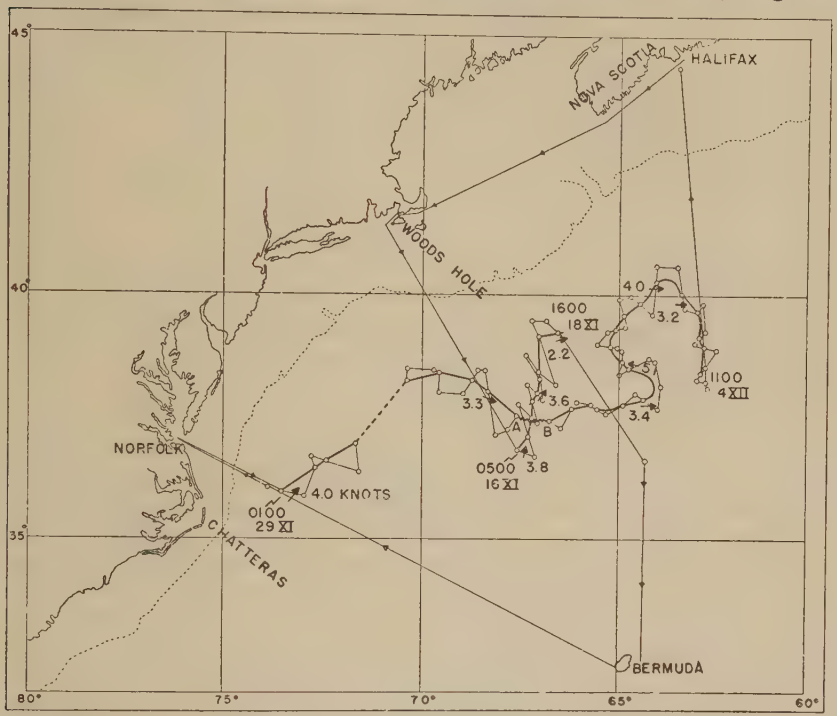


**Figure 1. Gulf Stream Cruise NL–16, Nov. 10 to Dec. 6, 1948. The heavy line is the "inshore" edge of the Stream. The light straight lines are the course of H. M. C. S. New Liskeard.**

and Worthington, 1947; Iselin and Fuglister, 1948; Seven BT Sections, Halifax to Bermuda 1946–47, six of which showed two or more crossings of the edge of the Stream; Naval Research Establishment, unpublished data). It is particularly interesting to note that this eddy and the one implied in the drift of the Valor are almost identical in size and location (Iselin and Fuglister, 1948). In 1945 the Valor drifted for ten days in this area and navigational records kept by Lt. D. T. Parsons, U. S. N. R., were sufficiently accurate to permit the construction of a current diagram which indicated the presence of a great anticyclonic eddy centered at 64° W. Long. and 39° N. Lat.

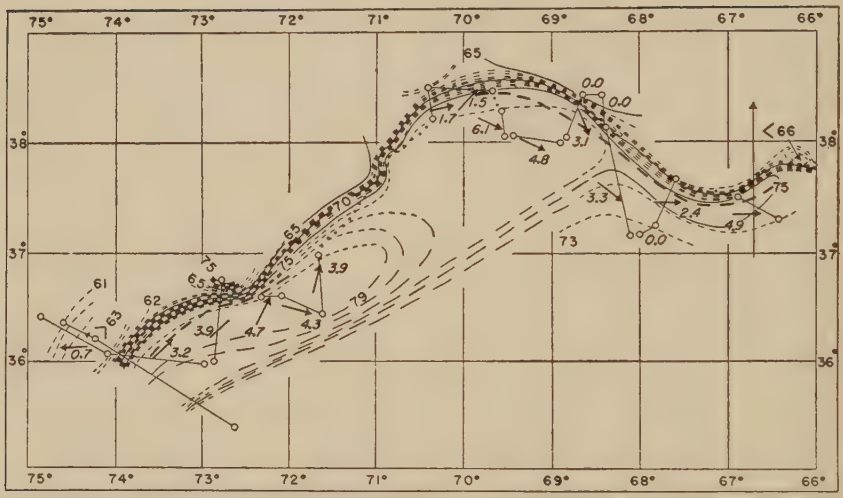


Figure 2. Surface temperature contours of a part of the Gulf Stream. The heavy dotted line is the edge of the Stream at a depth of approximately 150 feet. The arrows give the current direction and the adjacent numbers its speed in knots. The light straight lines are the ship's course.

To show surface temperatures and current velocities in necessary detail, the survey was divided into three parts, two of which are presented in Figs. 2 and 3. The third part, which is that section surveyed November 15–18, is omitted. The arrows give the direction of the current and the adjacent numbers show its speed in knots. The directions are the resultant of the vectors, dead reckoning course and true course, as determined by Loran fixes. The speed is the quotient of the resultant divided by the time. No allowance was made for wind drift. The fine straight lines give the actual ship's course as determined by Loran. The given velocities are averages for each leg. The terminals of the legs do not necessarily represent a change in compass course of the ship; in some cases they represent an alteration of the actual course by an abrupt change in current. Currents in excess of 5.5 knots were observed on several occasions. Although this method of determining surface current is crude, the data were carefully examined and it is believed that the above figure is reasonably correct. Fuglister and Worthington (1947) and others have also reported such values.

The vertical temperature distribution down to 800 feet was obtained by means of the BT every half hour during most of the cruise. Since it is impractical to present such a mass of data, a reasonably typical sample is presented in the form of two sections in Fig. 4.

Figure 3. Eastward continuation of Fig. 2.

The surface temperature characteristics of the Stream were as shown in Figs. 2 and 3. The warm core, with a maximum temperature of 80° F off Cape Hatteras, had cooled to less than 76° F on reaching 68° W. Long., but eastward of this point its temperature remained quite constant at 75 ± 0.5°.

The waters on the cold side of the front were mostly in the middle sixties except at the most northerly limits of the system. One such situation is shown in Fig. 3 at 64° W. Long., where a temperature of 50° F was found close to the front. Another similar case was found at 67° W. Long. and 39° 30′ N. Lat. during the earlier part of the survey. The nature of these cold waters will be discussed in the next section.

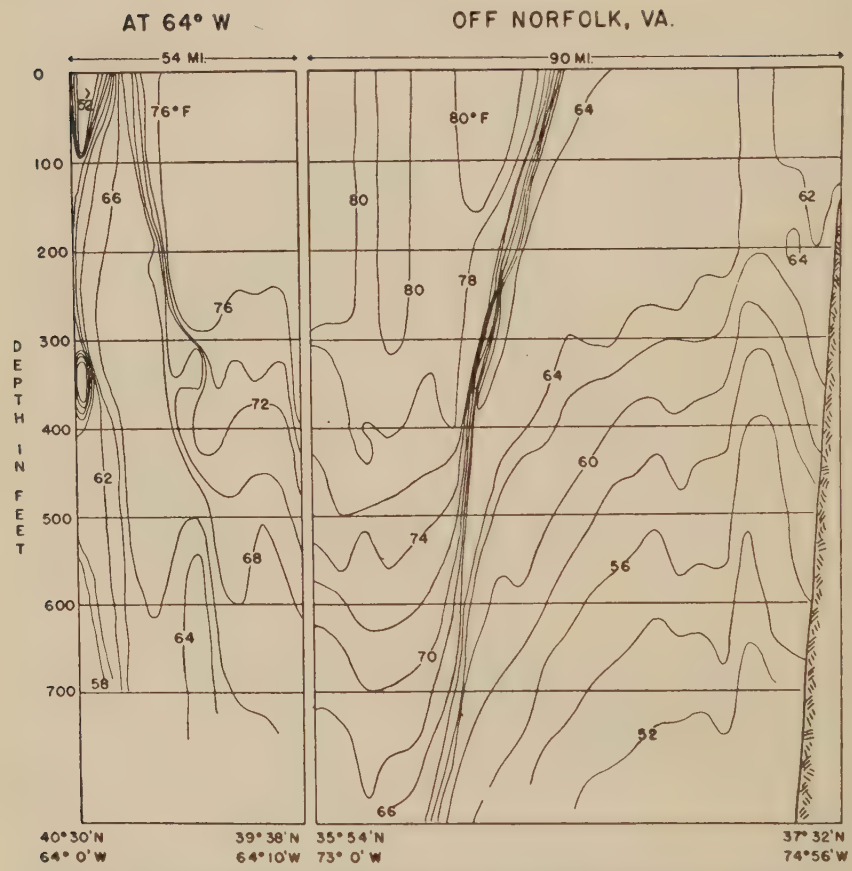


Figure 4. Two examples of B-T temperature sections showing the edge of the Stream.

## SURFACE WATER MASSES OF THE STREAM

A T-S analysis of the surface layer from data provided by the STD and the Sea Sampler has proven useful in developing a qualitative analysis of the water masses involved in the system. Such an analysis is subject to the criticism that the temperature under these conditions is not a conservative property but may in fact be subject to changes due to diurnal heating and cooling, meteorological changes, and seasonal trends. It is believed that the latter can be ignored, since the data were collected in a period of less than three weeks. The passage of weather would not be expected to produce serious errors because of the moderating influence of the ocean. Diurnal effects

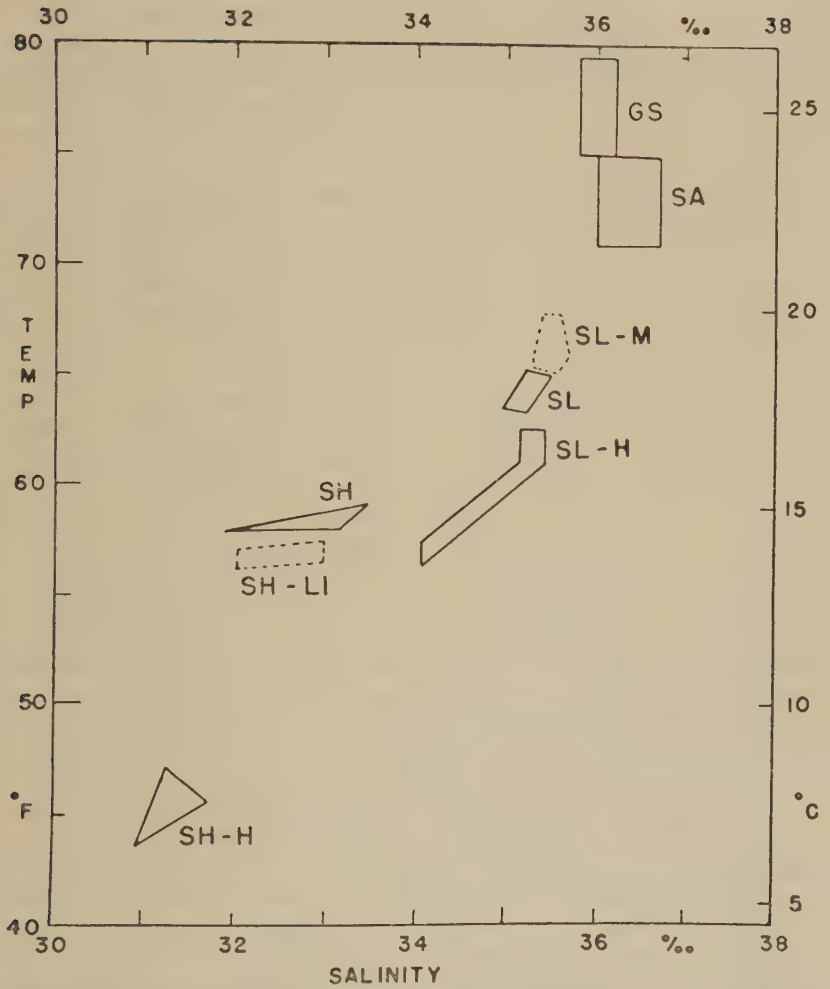


Figure 5. T-S relationships of the water masses of the surface layer of the Gulf Stream system. SH, SL and GS are respectively Shelf, Slope and Gulf Stream waters east of Norfolk, Va. SH-H and SL-H are respectively Shelf and Slope waters south of Halifax. SH-LI is Shelf water off Long Island. SL-M is Slope water south of Montauk Pt. SA is Sargasso Sea water. See text for details.

appear to be negligible, probably due to the low altitudes of the sun in November and December and to the turbulent character of the system. T-S diagrams showed a considerable scatter, which can be attributed in part to these factors and in part to the uncertainty ($\pm$ 0.2°/$_{oo}$) in the measurement of salinity by the STD. Nevertheless,

it is apparent that these uncertainties do not mask the main features. This is in agreement with Miller's (1950) conclusions on a similar use of T-S analysis. The main features are illustrated in Fig. 5, which is a T-S diagram that defines the surface water masses involved in this analysis. It provides a means of describing any given mixing zone in terms of two or more of these basic water types.

This diagram was obtained by plotting a large number of S-T observations taken from the STD record, and then, with the surface patterns of Figs. 2 and 3 in mind, those points which fell into characteristic groupings were enclosed in the manner shown. From a study of BT, STD and Sea Sampler records, it can be shown that these groupings, though necessarily somewhat arbitrary, represent reasonably homogeneous water masses.

Referring again to Fig. 5, Shelf water (SH) was defined as that which was found between 75° and 75° 30′ W. Long. on the course out from Norfolk, Va. Waters inshore of the latter point were not included, since they were of very low salinity and probably contained Chesapeake Bay outflow. Slope water (SL) was defined as that which lay between 74° and 74° 30′ W. Long. on the same course.

Gulf Stream water (GS) was defined by salinities and temperatures taken in the "core" of the Stream, in an area extending from off Cape Hatteras to about 66° W. Long. GS water is characterized by a salinity of $36 \pm 0.2$ °/₀₀ and by a temperature $> 75°$ F. Sargasso water (SA) was defined by observations taken on the course from the Gulf Stream towards Bermuda to about 35° N. Lat. and between Bermuda and Norfolk. It is characterized by a salinity $> 36.0$ °/₀₀ and a temperature $< 75°$ F. Surface water off Long Island (SH–LI) and surface Slope water south of Montauk Pt. (SL–M) are represented in a section from 71–72° W. Long. at 39° 50′ N. Lat. as reported by Miller (1950) for cruises of the Albatross III and Caryn in October and November 1948. Although these data were obtained one month before the New Liskeard cruise, they appear to be applicable to this analysis and are included to round out the picture. Furthermore, they are the only available data for this area, since no salinities were obtained in Cruise NL–16 on the run out from Woods Hole until 38° 30′ N. Lat. was reached. However, beyond this point, while still in Slope water, recorded STD salinities and temperatures fitted the SL–M grouping.

Slope water south of Halifax (SL–H) is a grouping based on observations taken on the return trip to Halifax between 40° N. Lat. and the 100-fathom line. It was the most difficult to define, and the grouping finally chosen appears to contain Shelf water—Halifax (SH–H). This latter water mass, quite clearly defined, represents the surface water as found while traversing the Scotian Shelf to Halifax.

A number of Sea Sampler stations have been analyzed to indicate the vertical extent to which the surface T-S analyses apply. The position of these stations are shown as circles in Figs. 6 and 7. Those Sea Sampler stations taken in the Stream (Nos. 3, 4, 6, 8, 10, 12, 13) show, with exception of No. 13, that the water was homogeneous from the surface down to 317 feet, the maximum depth of the Sea Sampler. No. 13 revealed homogeneous surface water (GS + SA) down to 200 feet and SA water below that. Sea Sampler stations taken in clearly defined Slope water (Nos. 2, 9, 14) showed a homogeneous water column to the maximum depth, 317 feet. The remaining stations (Nos. 1, 5, 7 and 11) were in boundary zones. No. 1 shows a homogeneous layer of SH + SL water 150 feet thick over SL water. No. 5 reveals a complex situation with a uniform mixture of GS + SH to 100 feet and then a transition layer passing through SL water at 200 feet to a higher salinity water at 250 feet. Nos. 7 and 11 show homogeneous mixtures of GS + SL and GS + SA + SL respectively to the maximum depth of the Sea Sampler.

In the open ocean, if a BT section reveals an isothermal surface layer, it is generally recognized that the layer is in fact also isohaline and may be considered homogeneous. The BT data of this cruise did show in general a mixed layer of more than 200 feet except in transition zones. Fig. 4 is an example that illustrates the point. On the basis of these considerations, it is assumed that surface salinities and temperatures represent an homogeneous layer, which was usually more than 200 feet thick throughout the area covered by the cruise. This statement, of course, is applicable only during the period of the cruise, since the mixed layer undergoes a seasonal variation, being deepest in midwinter and shallowest in midsummer.

In Figs. 6 and 7, the water masses described above are presented in their geographical relationship, and we may now see which water masses were involved in zones of mixing and how the system changed character from west to east.

The sections off Norfolk are of particular interest because of the presence of Shelf water (coastal) at the edge of the Stream. In Fig. 7 it will be seen that there was a narrow band of water of less than 63° at the edge of the Stream. Its T-S characteristics show that it was a mixture of SH and GS waters, mostly SH, and contained no SL water. The temperature section[2] (Fig. 4) suggests that it had a vertical extent of nearly 400 feet at the position of the section. The band was traced for about 80 miles along the edge of the Stream. The edge was not crossed again until a position some 140 miles further

[2] This diagram is uncorrected for temperature; correction is — 1.0° F.

along had been reached, and at this point, 70° 30′ W. Long., no evidence of Shelf water was found.

The presence of Shelf water along the edge of the Stream is explained by considering that the Shelf water flows southward on the continental shelf, turns eastward off Cape Hatteras and inserts itself between the Stream and the Slope water—eventually to be absorbed.

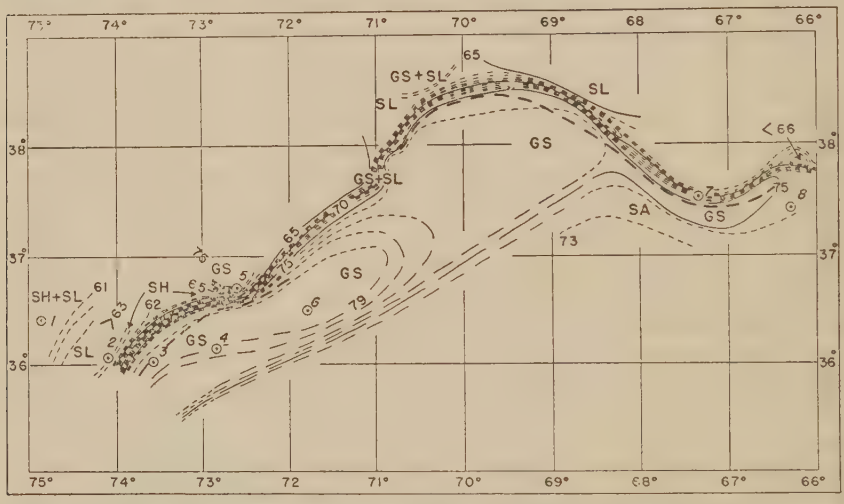


Figure 6. Surface temperature contours of a part of the Gulf Stream with the surface layer water types indicated. The numbered circles are Sea Sampler stations.

To strengthen this explanation, it is noted that the T-S characteristics of this water were such that it could not have risen from the depths; nor could it have come from coastal areas south of Hatteras. Hydrographic studies of that region in 1948 (Bumpus and Wehe, 1949) showed that there is little or no transport of Shelf water either north or south around Hatteras. These considerations agree with the concept that Cape Hatteras is a boundary zone between two distinct regimes upon the continental shelf. Therefore it is concluded that the low salinity water found at the edge of the Stream did originate on the shelf north of Hatteras.

It is of interest to note the appearance of SA water between the Stream proper and the 70° surface isotherm in the edge zone at several points within the great eddy. Consider, for example, a section through the edge at 63° 30′ W. Long. and 40° N. Lat. (Fig. 7). Beginning at a point to the north of the front and proceeding southward, the following waters were found: first a mixture of SH-H and SL-H, then a transition zone which included SL-H (35.5 °/₀₀ and 63° F),

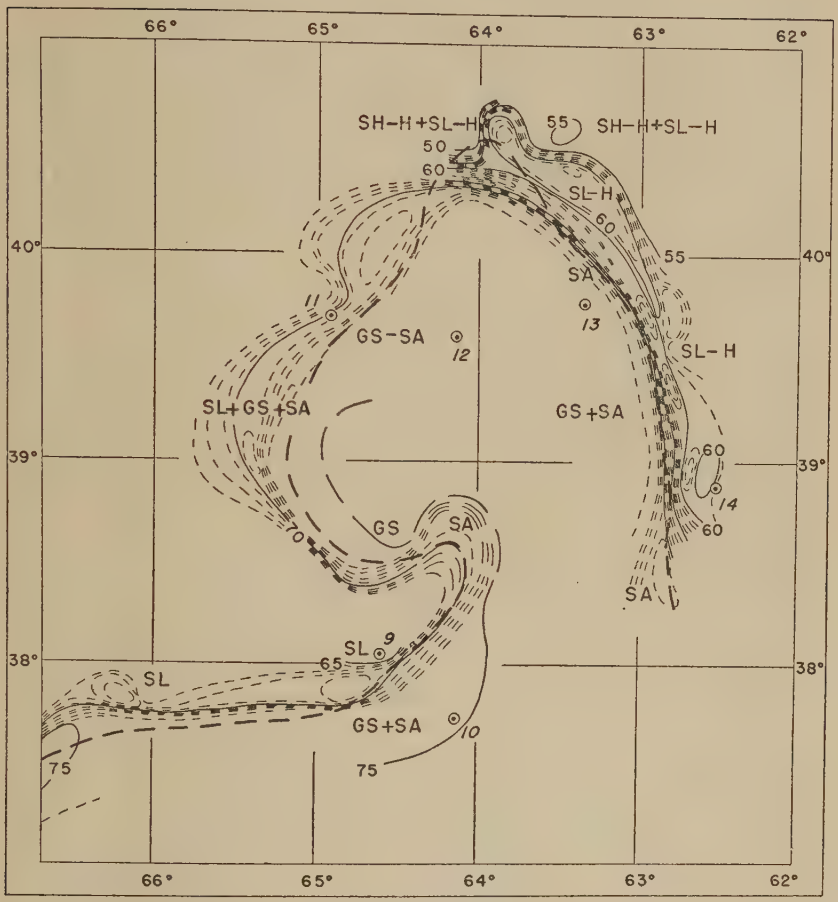


Figure 7. Eastward continuation of Fig. 6.

and then, very abruptly, SA water (36.25 °/₀₀ and 70° to 74° F). Next a gradual transition to a mixture of GS-SA waters (36.25 °/₀₀ and 75° F) was found. The density of the SA water is greater than that of the adjacent Stream but less than that of the Slope water.

Two interpretations as to the origin of this SA water may be considered: (1) it merely represents a mixture of GS-SA which has cooled a few degrees; (2) it actually represents SA water that had crossed the surface waters of the Stream at some depth and upwelled. Although there is not sufficient information to prove either point, the latter seems more acceptable. It has been shown that the SA water probably extends downward several hundred feet, and if this is so,

it is not likely that surface cooling could account for the lower temperature. Sea Sampler station No. 13 (Fig. 7), which was taken at the Gulf Stream end of the section discussed above, revealed SA water (70°–74° F and 36.4 °/₀₀) below a warmer and less saline surface layer, thus indicating the presence of a source for upwelling SA water.

At the most northerly reach of the Stream (Fig. 7), water of less than 55° F was encountered. This water proved to be a mixture of SH-H and SL-H waters. It is remarkable that Shelf water should be found so far offshore.

The T-S analysis shows the nature of the modification in the surface layer of the Stream as it flowed eastward. Downstream from Hatteras the temperature decreased, but there was no significant change in salinity and the water remained within the definition of GS water until 65° W. Long. was reached. In this neighborhood GS water as such disappeared (see Fig. 7) and was replaced by a mixture of GS-SA, which from this point on showed the general character of the water in the core of the Stream. That is to say, the surface salinity and temperature in the Stream proper, as recorded by the STD, fell in a narrow band encompassed by the GS and SA blocks as given in Fig. 5. It is clear also from Fig. 5 that if any appreciable amount of Slope water were included in the core of the Stream the T-S points would fall below the SA block. Such was not the case. In summary, as the stream moved eastward it appeared to be modified by the addition of Sargasso water. There appeared to be no absorption of Slope water.

Turning now to the Slope water adjacent to the Stream, the transition of its characteristics from west to east is shown in terms of T-S relationships in Fig. 5 and geographically in Figs. 6 and 7. Up to at least 65° W. Long. and 38° N. Lat. the Slope water is of the "Norfolk" type (SL). From this point to about 40° N. Lat. the ship's course did not extend far enough beyond the front of the Stream to clearly define the Slope water; but beyond this latter point, Slope waters adjacent to the Stream were of the "Halifax" type (SL-H). The two waters are outstandingly different in that the SL water was a homogeneous mass defined by a small range of salinity and temperature, whereas the SL-H water was found not as a clear-cut mass but in patches interspersed with mixtures containing water of the Scotian Shelf type (SH-H).

If that part of the SL-H block (Fig. 5) above 35 °/₀₀ is considered to be Slope water adjacent to the Gulf Stream, then SL-H and SL water differ only in temperature. Mere surface cooling could transform the latter into the former on the assumption of an easterly flowing Slope current adjacent to the Stream, as is postulated by Sverdrup, et al. (1942). On the other hand, if the Slope water adjacent to the Stream

moves westerly as a counter current, then the Slope waters in the westerly part of the area (SL) could result (Fig. 5) from the mixing of Stream water (GS–SA) with easterly Slope water (SL-H), providing it contains that part of the block below 35 °/₀₀.

The latter provides a more consistent interpretation, for when it is considered in conjunction with the evidence that the Stream absorbs Sargasso water but not Slope water, it leads to qualitative agreement with Rossby's (1936) wake stream theory. This theory requires that the Gulf Stream should absorb water from the oceanic areas to the right of the current and discharge water into a counter current on the left.

## ACKNOWLEDGMENTS

The cruise, initiated by the Naval Research Establishment of the Defence Research Board of Canada, was a joint effort with the Woods Hole Oceanographic Institution and the Atlantic Oceanographic Group, St. Andrews, N. B. The authors wish to acknowledge their indebtedness to: Mr. F. C. Fuglister of the Woods Hole Oceanographic Institution and to Mr. A. E. Calder of the Atlantic Oceanographic Group, upon whom, as members of the scientific party, the success of the cruise so largely depended; to the Commanding Officer, Lt. I. B. B. Morrow, R. C. N., and his officers and men of H. M. C. S. New Liskeard for their splendid cooperation; and to Mr. K. H. Hart of the Naval Research Establishment for his extensive aid in working up the large amount of data.

## REFERENCES

Bumpus, D. F. and T. J. Wehe
1949. Hydrography of the western North Atlantic; Coastal water circulation off the east coast of the United States between Cape Hatteras and Florida. Tech. Rep. Woods Hole oceanogr. Inst., No. 16, Ref. No. 49–6.

Church, P. E.
1937. Temperatures of the western North Atlantic from thermograph records. Ass. Ocean. Phys. Pub. Sci., No. 4: 1–32.

Ford, W. L.
1949. The field use of a salinity-temperature-depth recorder. J. mar. Res., *8* (1): 84–96.

Fuglister, F. C. and L. V. Worthington
1947. Hydrography of the western North Atlantic; Meanders and velocities of the Gulf Stream. Tech. Rep. Woods Hole oceanogr. Inst., No. 9.

Iselin, C.O'D.
1936. A study of the circulation of the western North Atlantic. Pap. phys. Oceanogr. Meteorol., *8* (1): 1–40.

Iselin, C.O'D. and F. C. Fuglister
1948. Some recent developments in the study of the Gulf Stream. J. mar. Res., *7* (3): 317–329.

Jacobsen, A. W.
1948. An instrument for recording continuously the salinity, temperature and depth of sea water. Trans. (mon.) Amer. Inst. elect. Engrs., *67:* 714–722.
Miller, A. R.
1950. A study of mixing processes over the edge of the continental shelf. J. mar. Res., *9* (2): 145–160.
Rossby, C. G.
1936. Dynamics of steady ocean currents in the light of experimental fluid mechanics. Pap. phys. Oceanogr. Meteor., *5* (1).
Spilhaus, A. F.
1940. A detailed study of the surface layers of the ocean in the neighborhood of the Gulf Stream with the aid of rapid measuring hydrographic instruments. J. mar. Res., *7* (1): 51–75.
1941. Fine structure of the edge of the Gulf Stream. Trans. Amer. geophys. Un., 22nd Annu. Meeting, Part II: 478–484.
Spilhaus, A. F. and A. C. Miller
1948. The sea sampler. J. mar. Res., *7* (3): 370–384.
Sverdrup, H. U., M. W. Johnson and R. H. Fleming
1942. The Oceans. Prentice-Hall, Inc., New York. p. 679.

# ON THE NATURE, OCCURRENCE AND ORIGIN OF COLD LOW SALINITY WATER ALONG THE EDGE OF THE GULF STREAM[1]

By

W. L. FORD, J. R. LONGARD and R. E. BANKS

## ABSTRACT

In the left margin of the Gulf Stream, looking in the direction of flow, a narrow discontinuous band of relatively cold water is often found. This has been attributed to upwelling from the colder depths of the ocean, but recent investigations throw doubt on this explanation, since this water, which forms a thin layer close to the surface, may have a lower salinity than any water in the depths. Evidence is given that the only cold low salinity source is the so-called Shelf water, which is found in a broad band between the shore and a boundary off the Continental Shelf.

It is shown that the cold low salinity water in the margin of the Stream, when mixed with the warm high salinity water of its core, may form a product which is identical to the Slope water which lies between the Gulf Stream and the Shelf. It is postulated that this product is discharged to the left of the Stream to form a source of the upper layer of Slope water.

## INTRODUCTION

It has been recognized for some time that unexpectedly cold water occurs at the surface along the left-hand edge of the Gulf Stream, but beyond this the phenomenon has received little attention. On the basis of thermograph records from merchant ships, Church (1937) reported that the temperatures on the northern edge are often a degree or more (°C) below those on either side and that sometimes these low temperatures are not matched within 40–80 miles to the north. He noted also that the occurrence is quite consistent during the colder half of the year but less so during the warmer half.

Spilhaus (1940) reported results of the first detailed study of the edge of the Stream, made possible by the Bathythermograph (BT) and Sea Sampler. A feature of his observations was the presence of a cold layer, with minimum temperature at about 200 feet, immediately adjacent to the warm water of the Stream; he attributed this cold layer to upwelling. The salinity observations obtained with the Sea Sampler did not happen to embrace the cold layer, and if they had, it is probable that remarkably low salinity values would have been obtained, too low in fact to be explained by upwelling from the depths, which contain water of relatively high salinity.

[1] This paper is a contribution from the Naval Research Establishment of the Defence Research Board of Canada, Halifax, N. S.

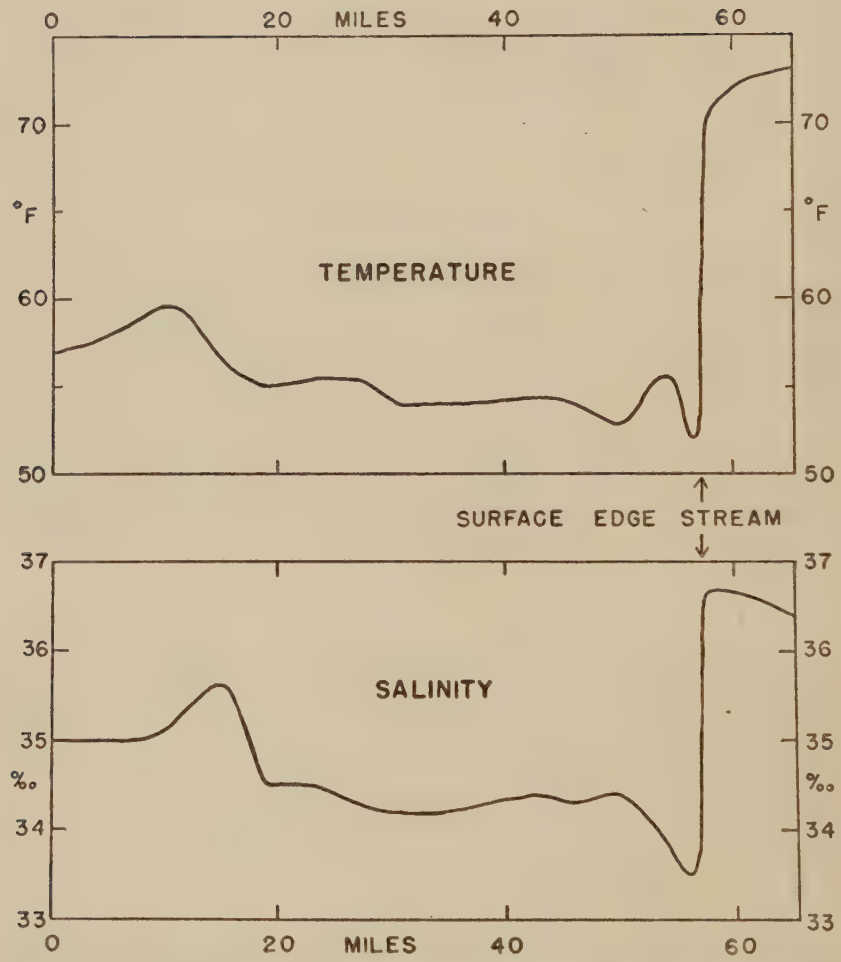


Figure 1. A plot of continuous surface temperature and salinity recordings from the STD in a crossing of the edge of the Gulf Stream at 37° 20′ N. Lat. and 71° 35′ W. Long., ATLANTIS Cruise 137, December 13-14, 1945. Corrected values have been plotted. The main features in the curves are considerably larger than the uncertainty in the data, which for salinity is approximately ± 0.15 °/₀₀, for temperature ± 0.2° F.

With the advent of detailed BT surveys of the Stream, accompanied on occasions by continuous recordings of the surface salinity and temperature by means of a Salinity-Temperature-Depth Recorder (STD), the temperature phenomenon was repeatedly observed (Jacobsen, 1948; Ford, 1949). The STD has shown that the temperature dip may be accompanied by a drop in salinity, sometimes to

values lower than any observed in the Slope water to the north. An interesting example of this is given in Fig. 1, obtained during the first ocean cruise in which the STD was used.

Ford and Miller (1952), in a survey of the Stream in 1948 with the BT, STD and Sea Sampler (Spilhaus and Miller, 1948), noted the occurrence of cold water at several points along the Stream. It was shown that one occurrence of it, located just to the northeast of Cape Hatteras, originated from the Shelf or coastal water.

It is the purpose of this paper to examine the nature, frequency of occurrence, and origin of such cold low salinity water. Since the multiple ship survey of June 1950, "Operation Cabot," provided such exceptionally good coverage of the Gulf Stream, this paper is based for the most part on data from that survey. The reader is referred to a paper by Fuglister and Worthington (1951) for a description of the operation. It is to be noted that the present analysis is a by-product of the multiple ship survey and of previous surveys; it was not considered in the planning and execution stages. As a consequence, the character and amount of data available, particularly on salinity observations at depth, leave much to be desired.

## THE NATURE OF THE WATER

The nature of the cold water can best be described by a detailed inspection of an example in which the phenomenon was not only well developed but for which relatively complete data were obtained. The surface characteristics are illustrated in Fig. 2. It shows how cold water may be found as a band at the edge of the Gulf Stream, which in this case is approximately defined by the 70° F isotherm.

In order to illustrate the structure and depth of the cold band, sections AA and BB in Fig. 2 are presented in vertical profile in Figs. 3A and 3B. The outstanding feature is the presence of a thin cold layer with minimum temperature at a depth of about 200 feet. The layer extends under the warmer surface water of the Stream. It is not only cold, but it has a very low salinity, as shown by three plots of temperature and salinity against depth in Fig. 4. The T-S diagram in the lower part of Fig. 4 emphasizes this point and shows that the cold low salinity water (curve 2) has quite different characteristics from the waters on either side of it. Of the many sea sampler and hydrographic stations made during Operation Cabot, only four produced samplings directly through the cold layer. In each of these the same T-S pattern was observed.

It will be assumed that a cold low salinity layer exists if a temperature inversion with a minimum of less than 55° F occurs in the upper

600 feet. From analysis of the available salinity data on cold layers, this rather arbitrary upper limit appears to be a conservative one. Temperature inversions greater than 55° F were not considered, since too little is known of their salinity to have any confidence that they could be identified properly.

In Figs. 3A and 3B it will be seen that a tongue of the cold low salinity water extends to the surface and is reflected in the surface temperature and salinity plot. Although this sample is quite typical,

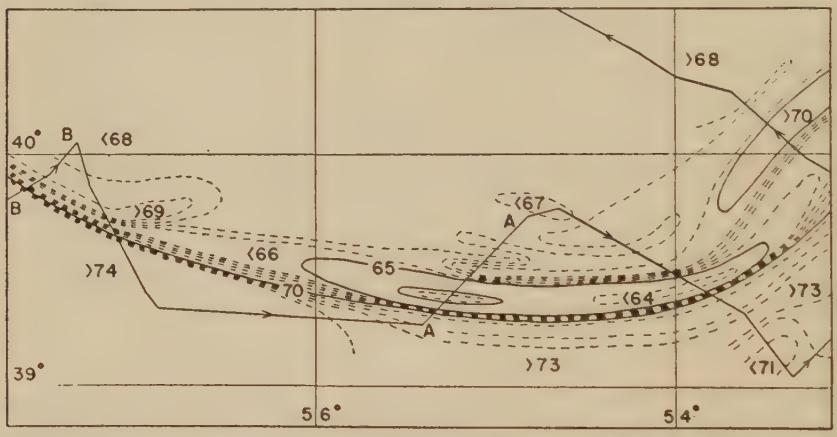


Figure 2. Surface temperature contour plot from STD data of H. M. C. S. New Liskeard. Ship's course is shown as arrowed lines. Sections AA and BB cross the Stream at an angle of about 60° to the current which parallels the isotherms.

not all cold layers exhibit this surface manifestation. Thus, of 19 consecutive crossings of the Stream made by H. M. C. S. New Liskeard between 64° and 51° W. Long. during Operation Cabot, eight contained a subsurface cold layer, only five of which gave a significant dip of surface temperature and salinity as observed by the STD. On the other hand, six of the 19 crossings showed a marked drop in surface values in the absence of a subsurface cold layer. In these cases a narrow cold layer might have been present between successive BT observations, or the recorded minimum temperature might not have been as low as 55°. The decrease in surface salinity and temperature with reference to the relatively steady values observed in nearby Slope water varied between 0.4 and 2.2 °/₀₀ and 1° and 6° F, respectively.

Figure 3. Details of Sections AA (3A) and BB (3B) of Fig. 2. Upper section of each gives surface temperature and salinity from STD and the uncorrected surface velocity component normal to the ship's course from GEK. Lower sections give the temperature profiles from BTs.

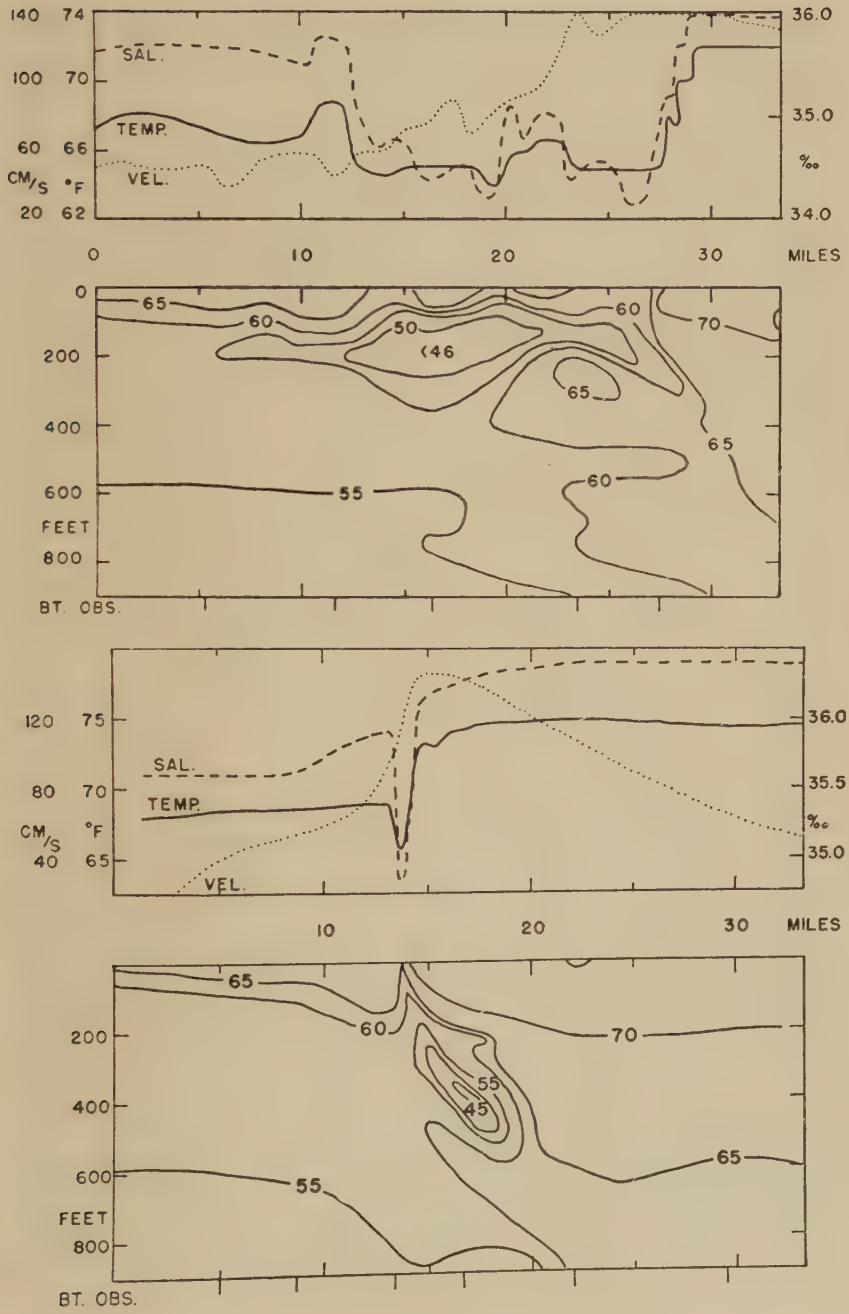
140 74
SAL.
100 70
TEMP.
60 66
CM/S °F
VEL.
20 62
36.0
35.0
‰
34.0
0
10
20
30
MILES
0
65
60
50
46
60
70
200
65
400
65
600
55
60
FEET
800
BT. OBS.
120 75
SAL.
80 70
TEMP.
CM/S °F
40 65
VEL.
36.0
35.5
‰
35.0
10
20
30
MILES
65
60
70
200
55
45
400
65
600
55
FEET
800
BT. OBS.

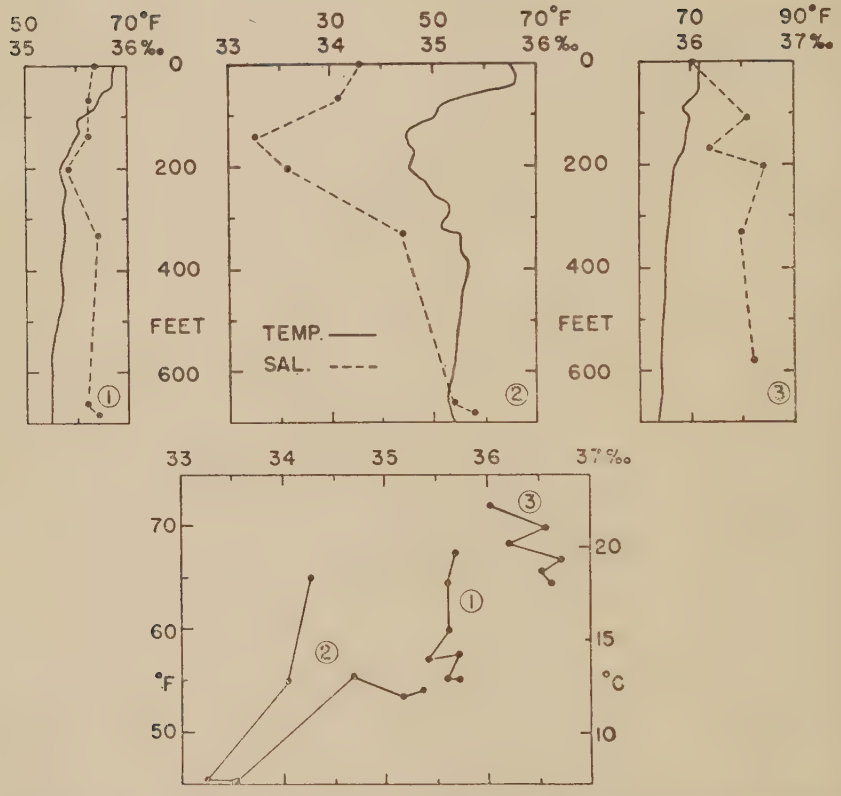


Figure 4. Temperature and salinity plots for three Sea Sampler lowerings through Section AA. No. 1 is the water outside the Stream (Slope water); No. 2 is the water through the middle of the cold layer (centre of Fig. 3A); and No. 3 is in the Gulf Stream.

There is evidence that the cold water in the margin of the Stream is in fact a part of the current. On approaching the Stream it may be seen (Fig. 3B) that the surface temperature and salinity have started to rise and that the depth of the surface layer has increased before the cold water is reached, and, in the absence of the cold water, the 65 and 60° isotherms might well have joined across the space occupied by it. The velocity curve shows that the surface cold water is within the Gulf Stream current, from which it may be inferred that the cold water mass below is also entrained in the current. From the surface salinity and temperature recordings the densities of the surface waters have been computed. The density of the cold water is intermediate between waters of the Slope and Gulf Stream.

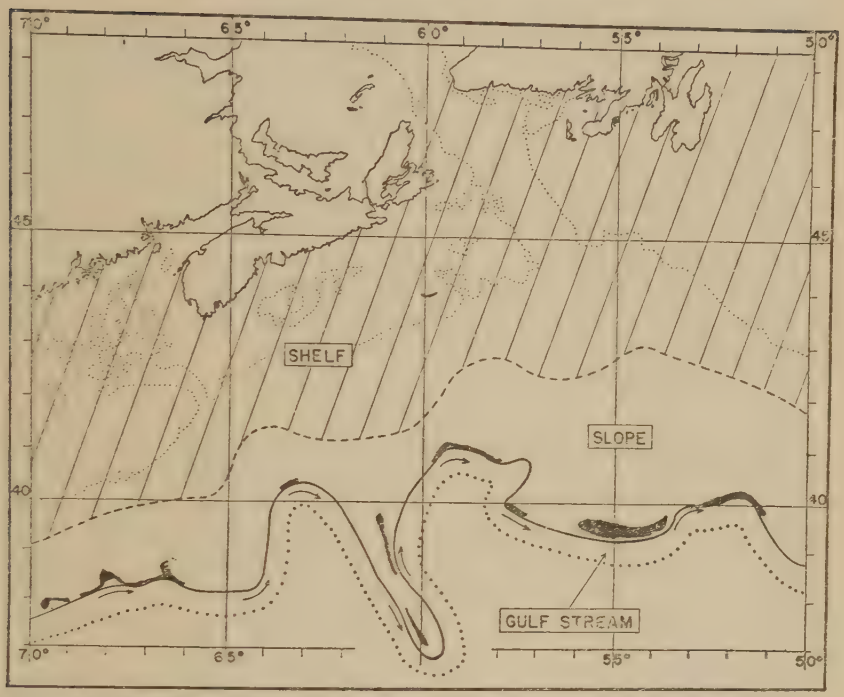


Figure 5. Distribution of temperature inversions with minima less than 55° F in the upper 200 m along the edge of the Stream during the first eight days of operation Cabot (cross hatched). Approximate southern limits of Shelf water at this time are indicated by dashed line.

It may be noted also in Figs. 3A and 3B that the cold water reached the surface at the point of maximum velocity gradient, as measured by the geomagnetic electro-kinetograph (GEK). Von Arx (1951) has shown that this is a region of maximum shear and, as in these cases, is usually close to the point of maximum velocity. He has also shown that slicks are associated with such shear regions, and, on at least one occasion, we observed that the slick water was colder and of lower salinity than the adjacent ruffled water. Thus, such slicks may well be surface evidence of subsurface cold layers.

## FREQUENCY OF OCCURRENCE

The BT profiles for the area east of 70° W. Long. obtained by five of the ships involved in Operation Cabot have been examined and the occurrence of cold layers noted. Exclusive of the large eddy "Edgar" and its connecting neck, there were 97 crossings of the edge of the Stream; 57 crossings contained cold layers, of which 19 had a temperature minimum of less than 50° F.

Fig. 5 shows the distribution of the cold strips found in the first eight days of Operation Cabot. Similar charts have been prepared for the second half of this operation and for several other Gulf Stream surveys. It is clear that the cold layer, as defined above, occupies only fractional parts of the Stream's length and is therefore not a continuous band along the Stream. Whether so-called "diluted remnants" tend to fill in the gaps to form a continuous band is a question that must await further surveys for which special sampling techniques will be required. The presence of temperature inversions in almost all BT plots across the edge of the Stream as well as points of temperature and/or salinity inversions in certain of the hydrographic stations from Operation Cabot suggest that "diluted remnants" can be recognized.

## ORIGIN

In order to discuss the origin of the cold layer, three water types, Shelf, Slope and Gulf Stream, will be defined in terms of their T-S relationship as shown in Fig. 6. For the purposes of this paper the terms apply to the surface layer above 200–300 m. Below 200–300 m for the Gulf Stream and about 100 m for the Slope, the T-S curves become indistinguishable from the well established curve for Central Atlantic Water (Iselin, 1936; Pollak, 1947), shown as a heavy black curve in Fig. 6.

The approximate spatial relationships of these waters in early June 1950, i. e., during the first half of Operation Cabot, are shown in Fig. 5. The term Shelf has been applied to all of the relatively cold and low salinity water between the shore and a boundary separating it from Slope water. It is preferred to the term Coastal, which has been used in the literature, since the water in question is hardly coastal, extending, as it does, well beyond the Continental Shelf. The boundary between Shelf and Slope was taken as the seaward limit of the Shelf cold layer, which limit was found to be coincidental with the 50° isotherm. The Shelf boundary is drawn on the basis of six separate BT sections between 50 and 70° W. Long., made during the first half of June 1950. The Gulf Stream is essentially as given by Fuglister and Worthington (1951).

The T-S plots are based on data from Operation Cabot, with the exception of those for the Shelf, which include data collected during May, July and August 1950, since there was insufficient coverage for June alone. The restriction of the data to a short period of time is necessary since T-S relationships cannot be applied satisfactorily to surface layers in which seasonal changes have occurred.

The Gulf Stream and Slope envelopes contain approximately 250 observations of temperature and salinity from hydrographic stations

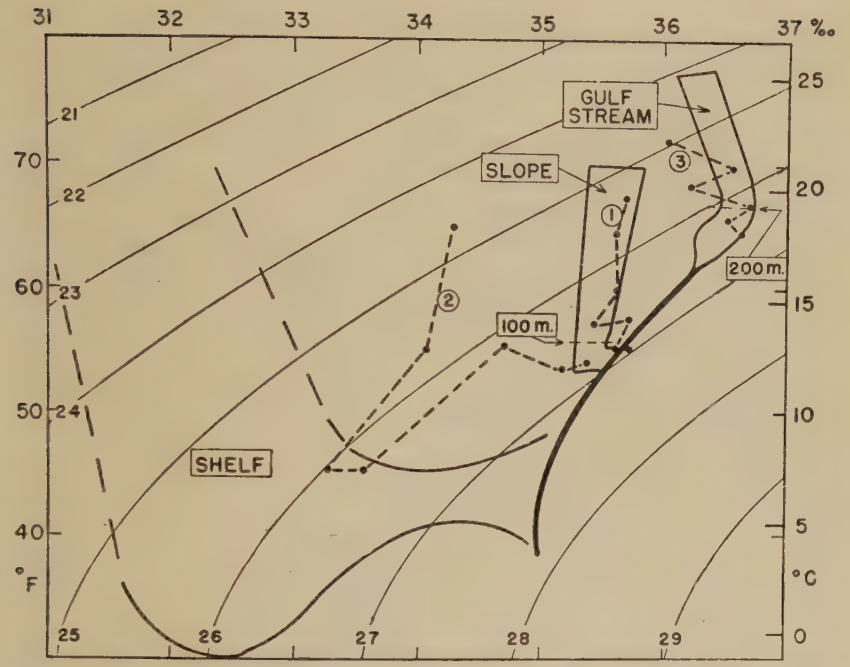


Figure 6. T-S envelopes of Gulf Stream, Slope and Shelf waters. Surface layer Shelf water is shown dashed. Curves 1, 2 and 3 are those of Fig. 4, indicating cold water of No. 2 to be of Shelf water origin.

and sea sampler lowerings distributed over the area under consideration. Only those observations that were definitely in the Gulf Stream or in the Slope were used. The Shelf envelope is based on 140 observations.

Also plotted in Fig. 6 are the T-S curves of Fig. 4 which result from three Sea Sampler lowerings made (1) north of the Stream, (2) in the edge of the Stream, and (3) in the core of the Stream. Curves (1) and (3) fall approximately within the envelopes for Slope and Gulf Stream waters. However part of curve (2) falls within the envelope for Shelf water. Thus it seems quite evident that the Shelf water in this case is the source of the cold low salinity layer found in the edge of the Gulf Stream.

By definition the cold water considered in this paper is marked by a temperature inversion in the upper 200 m. The presence of such an inversion suggests that there is also a corresponding salinity inversion, in accordance with T-S diagram relationships; otherwise a condition of extreme density anomaly and consequent instability must be

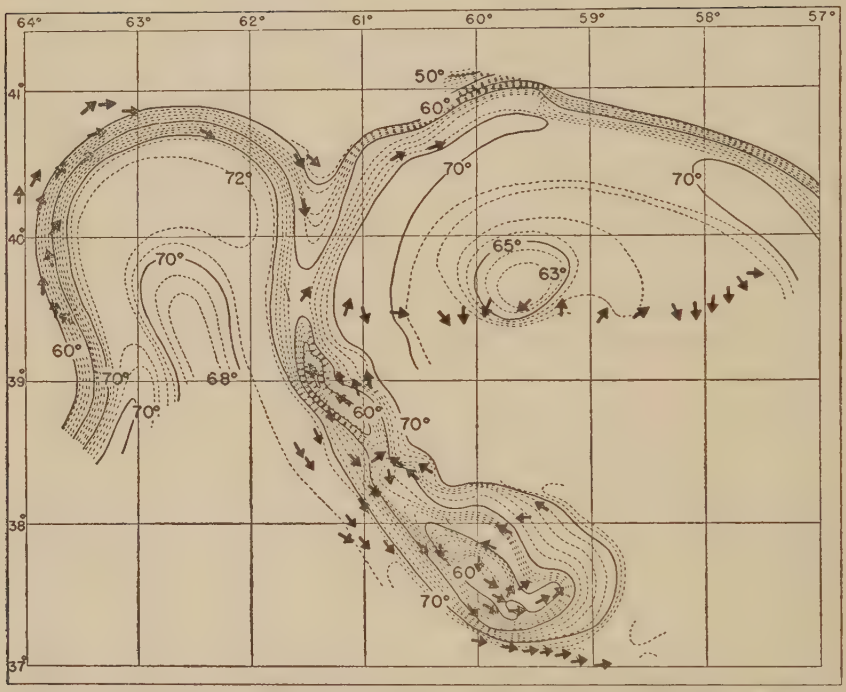


Figure 7. Plot of average temperatures in upper 200 m in vicinity of "Edgar" on June 17, showing cold water in neck and main body of eddy. Current arrows are from G. E. K. From Fuglister and Worthington (1951) by courtesy of Tellus and the Woods Hole Oceanographic Institution.

postulated. The minimum salinity to be found in the depths below the Stream and adjacent waters is 34.9 °/₀₀. From T-S diagrams, temperatures below 50° F found in the upper 200 m should be associated with salinities considerably less than 34.9 °/₀₀ if density anomalies are to be avoided. Hence, in the few cases for which salinity samples were obtained and also in the many cases where temperatures only were available, cold layers with temperatures in the vicinity of 50° F found in the upper 200 m must be of Shelf water origin rather than the result of upwelling.

## THE COLD CORE OF THE EDDY AND ITS NECK

So far we have dealt only with crossings of the Stream exclusive of the eddy. The position of this eddy and the cold water found near its centre and in the neck during the period June 8–13 is indicated in Fig. 5; for a later stage of the development of the eddy, June 17, see Fig. 7, reproduced here by courtesy of Fuglister and Worthington

(1951). Although Fig. 7 gives the average temperature of the upper 656 feet (200 m), the BT records show that the cold water masses were associated as usual with temperature inversions within this depth.

The only hydrographic station to sample the cold core of the eddy or its neck was that made by U. S. S. San Pablo on June 14 in the eastern edge of the cold water of the neck. The minimum salinity observed was 34.7 °/₀₀ with a temperature of 56° F at 230 feet. Several records of abnormally low surface salinities were obtained from STD records by both the Atlantis and H. M. C. S. New Liskeard. In the area of the cold core of the neck of the eddy (see Fig. 7) from June 5 to 17, both ships observed surface salinities of 33.0 °/₀₀ at a temperature of about 60° F in association with a well defined cold layer in which temperatures of less than 50° F, minimum 43°, extended between 250 and 550 feet. In the main body of the eddy on June 19, i. e., after it had split off from the Stream, New Liskeard recorded a surface salinity minimum of 32.9 °/₀₀ at a temperature of 62° F in association with a cold layer whose minimum temperature was 43° F centred at 425 feet. Also, in other sections in this area both ships observed surface salinity minima of 34.5 °/₀₀ located above well defined cold layers containing water colder than 55°. Temperature profiles for these cases, showing upward extension of cold water to the surface, are quite parallel to those shown in Figs. 3A and 3B.

As in the main Gulf Stream, such cold low salinity water can be only of Shelf origin, and with the splitting off of the eddy, which occurred toward the end of Operation Cabot, this Shelf water was in a remarkable position, namely in the Sargasso Sea, seaward of the Gulf Stream.

## DISCUSSION

It is of interest at this point to discuss what part the cold low salinity strips may play in maintaining the temperature and salinity characteristics of the system. Consider first certain aspects of the dynamics of the system as given by Rossby (1936), who has shown from theoretical consideration that the Gulf Stream on its eastward path assimilates water from its right side (i. e., from the high salinity mass of the Sargasso Sea) and discharges it on its left side (i. e., into the lower salinity Slope water) and that there should be a Slope counter current adjacent to the Stream. Supporting experimental evidence of this lateral transport from right to left is given for the surface layer by Ford and Miller (1952) and by data from Operation Cabot, during which the upper 200 m was repeatedly sampled, both in the Stream and in the nearby Slope from 66° to 50° W. Long., a distance along the Stream of over 800 miles. From west to east there was a significant shift in the surface layer of the Stream towards higher

salinity (+ 0.2 °/₀₀) and lower temperature (− 3° F) which suggests the absorption of water from the more saline cooler area to the right. On the other hand *no* significant change in the T-S characteristics of the Slope water was observed. In support of Rossby's prediction of a counter current, Fuglister (1951) gave a plot of the 200 m temperature contours based on all available data; this plot indicates a counter movement of Slope water running adjacent and parallel to the Stream.

If cold low salinity water is introduced into this system and if it is assumed that it is entrained in the current and consequently mixes mainly with Gulf Stream water, the resulting product will be discharged into the Slope area in accordance with the theory. From the mixing relationships evident in the T-S diagram in Fig. 6 it follows that this product can have the properties of, and may be a source of, Slope water. Such a product is not only possible but necessary. If the Rossby process is considered as operating in the absence of this product, then the discharged Gulf Stream water would cause a progressive change towards higher salinity and temperature in the Slope water counter current from east to west. Such, however, is not the case. In fact, as mentioned above, the T-S characteristics of the surface layer of the Slope water are unchanged over a considerable distance alongside the Stream.

## REFERENCES

Church, P. E.
1937. Temperatures of the western North Atlantic from thermograph records. Ass. Ocean. Phys. Pub. Sci., No. *4:* 1–32.

Ford, W. L.
1949. The field use of a Salinity-Temperature-Depth Recorder. J. mar. Res., *8* (1): 84–96.

Ford, W. L. and A. R. Miller
1952. The surface layer of the Gulf Stream and adjacent waters. J. mar. Res., *11* (3): 267–280.

Fuglister, F. C. and L. V. Worthington
1951. Some results of a multiple ship survey of the Gulf Stream. Tellus, *3* (1): 1–14.

Fuglister, F. C.
1951. Multiple currents in the Gulf Stream system. Tellus, *3* (4): 230–233.

Iselin, C.O'D.
1936. A study of the circulation of the western North Atlantic. Pap. phys. Oceanogr. Meteorol., *8* (1): 1–40.

Jacobsen, A. W.
1948. An instrument for recording continuously the salinity, temperature and depth of sea water. Trans. (mon.) Amer. Inst. elect. Engrs., *67:* 714–722.

Pollak, M. J.
1947. On the hydrography of the western Atlantic; Hydrography of the subsurface slope water. Tech. Rep. Woods Hole oceanogr. Inst., No. 5.

ROSSBY, C. G.
1936. Dynamics of steady ocean currents in the light of experimental fluid mechanics. Pap. phys. Oceanogr. Meteorol., *5* (1): 1–26.
SPILHAUS, A. F.
1940. A detailed study of the surface layers of the ocean in the neighbourhood of the Gulf Stream, with the aid of rapid measuring instruments. J. mar. Res., *3* (1): 51–75.
SPILHAUS, A. F. AND A. R. MILLER
1948. The sea sampler. J. mar. Res., *7* (3): 370–385.
VON ARX, W.
1951. Some measurements of the surface velocities of the Gulf Stream. Tech. Rep. Woods Hole oceanogr. Inst., Ref. No. 51–96.

## ERRATA

JOURNAL OF MARINE RESEARCH
(Volume XI, Number 2)

Page 106, last sentence of the first paragraph in the ABSTRACT should read:

"The salinity is on the average *lower* on the right side of the estuary (looking downstream) than on the left.

## NOTE TO AUTHORS

The pages of this Journal are open to all contributors, and manuscripts may be submitted to any member of the Board of Editors or to the Managing Editor. Publication will be made only in the English language, but copy may be submitted for consideration in other languages. Aid in translation of accepted manuscripts will be given when possible.

All manuscripts should be typewritten with double space, carefully corrected, with footnotes continuously numbered and set off in the body of the text. If an article is to appear as a contribution from another institution, it should be approved by that institution before submission; contribution numbers of such institutions are submitted with the return of galley proofs.

The author (or authors) of each article will receive a total of 50 free reprints (with covers). Additional reprints with or without covers may be ordered by authors or institutions at the cost of printing. Orders for reprints are given when galley proofs are returned.

Both galley and page proofs are submitted to the senior author of each article.

Tables should be prepared for clarity and as near as practicable to Journal pattern, without ruled lines if possible. Table footnotes should appear at the base of each Table.

Figures are required for consideration simultaneously with the manuscript. Original figures of inconvenient size for forwarding may be represented by photographs on first submission of a manuscript; originals are required for line cuts. Illustrations requiring half-tone reproduction should be avoided as far as possible, but they will be accepted when necessary. *It is very important that the proper size of characters and symbols should be used for the lettering of illustrations.* A diagram for determining suitable heights of letters for original drawings that will be reduced, together with an explanatory note, has been published in this Journal, Vol. III, No. 1: 89–91; reprints will be submitted to authors on request. Mechanical lettering is recommended. If facilities for lettering are not available to the author, it is preferable to receive illustrations with lettering indicated in pencil only, to be finished in ink in the editorial office. All illustrations will be subject to at least a minimum reduction at the rate of 1 : 1.2. Drawings which have been heavily patched and pasted must *not be rolled* for mailing. The legends for the figures, identified by corresponding figure numbers on the illustrations also, should be typed in sequence at the end of the manuscript.

*A complete* and *accurate list of references* in alphabetical order at the end of each article is essential. References may be indicated in the text by author's name (or names) and *year of publication*, or by italicized numbers which correspond to the numbers given in sequence in the list of references. Each reference should include the last name followed by at least two initials or first name; co-authors should be listed with the initials or first name preceding the last name. The date should be indented on the line below, followed by a complete title *verbatim* in lower case except for the first word. Publisher, city and pagination should be indicated for books; for periodicals (abbreviations from "World List of Scientific Periodicals," Oxford, as far as possible), the volume (italicized), number and pagination should be given.

Additional information regarding the preparation of manuscripts will be furnished by the Managing Editor.

TABLE OF CONTENTS

Page

1. **M. S. Longuet-Higgins:** On the statistical distribution of the heights of sea waves ..... 245

2. **W. L. Ford and A. R. Miller:** The surface layer of the Gulf Stream and adjacent waters ..... 267

3. **W. L. Ford, J. R. Longard and R. E. Banks:** On the nature, occurrence and origin of cold low salinity water along the edge of the Gulf Stream ..... 281

4. **Errata** ..... 293